

Atomic Physics Notes

Flo Brimcombe

June 30, 2025

1 Lecture 1

Consider a 2 level atom in a field of monochromatic EM radiation. The evolution of the system can be described in terms of time dependent coefficients of the eigen-states of a columbic Hamiltonian.

$$\Psi(\vec{r}, t) = c_1(t)\psi_1(\vec{r}) \exp\left(-\frac{iE_1 t}{\hbar}\right) + c_2(t)\psi_2(\vec{r}) \exp\left(-\frac{iE_2 t}{\hbar}\right) \quad (1)$$

We determine each $c_i(t)$ through substituting (1) into the time dependent Schödinger equation:

$$i\hbar \frac{\partial \Psi}{\partial t} = \hat{H}\Psi \quad (2)$$

The Hamiltonian takes the form:

$$\hat{H} = H_0 + e\vec{r} \cdot \vec{E}_0 \cos(\omega t) \quad (3)$$

Here, the second part represents the potential energy of an electric dipole created through and induced misalignment between the electron cloud and nucleus. \vec{r} is the position of the electron with respect to the atom's center of mass. Once the substitution has been simplified, we take an inner product of the result with each $\langle \psi_1 \rangle$ and $\langle \psi_2 \rangle$ respectively.

The Rabi frequency is introduced:

$$\Omega = \frac{\langle 1 | e\vec{r} \cdot \vec{E}_0 | 2 \rangle}{\hbar} \quad (4)$$

The evolution of the system is then described by the following first order, coupled differential equations (we have made the rotating wave approximation):

$$i\dot{c}_1(t) = \frac{\Omega}{2} \exp(i(\omega - \omega_0)t) c_2 \quad (5)$$

$$i\dot{c}_2(t) = \frac{\Omega^*}{2} \exp(-i(\omega - \omega_0)t) c_1 \quad (6)$$

The system is solved through obtaining the second order differential equation:

$$\ddot{c}_2 + i\dot{c}_2(\omega - \omega_0) \frac{|\Omega|^2}{4} c_2 = 0 \quad (7)$$

which is solved by applying the boundary conditions $c_1(t=0) = 1$, $c_2(t=0) = 0$ and through defining W for simplicity.

$$W = \sqrt{|\Omega|^2 + (\omega - \omega_0)^2} \quad (8)$$

$$|c_2|^2 = \frac{|\Omega|^2}{W^2} \sin^2\left(\frac{Wt}{2}\right) \quad (9)$$

W is the effective Rabi Frequency; as $\omega \rightarrow \omega_0$, $W \rightarrow \Omega$. The system evolves as an oscillation between states, see Figure (1). On resonance ($\Delta = 0$), the maximum of $|c_2|^2$ is 1, hence we transfer all atoms to the excited states at certain times. Away from resonance ($\Delta \neq 0$) we reduce the amplitude of $|c_2|^2$ and increase the frequency of oscillation.

For $\Delta = 0$ we obtain a fully excited state at $\Omega t = \pi$ and a 50-50 superposition at $\Omega t = \frac{\pi}{2}$.

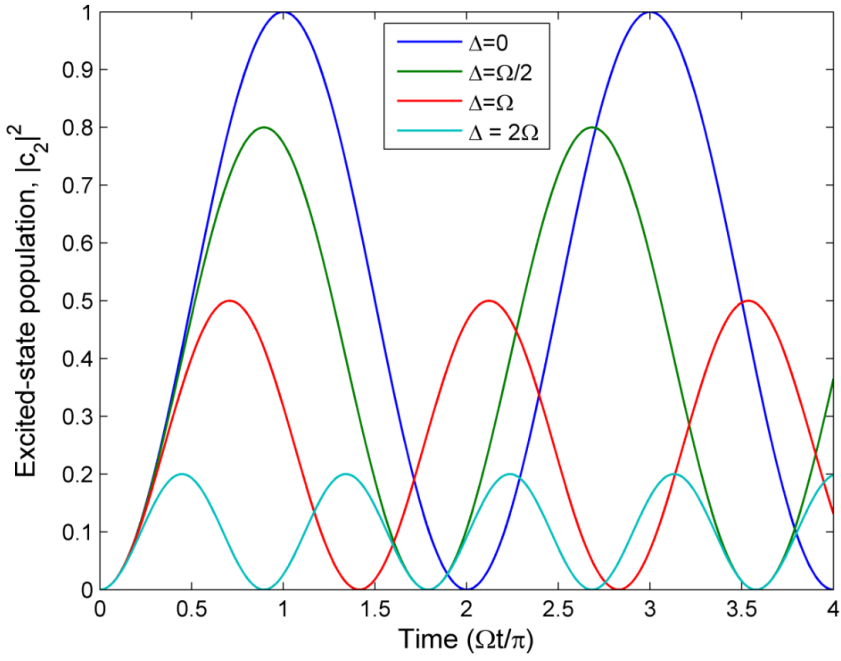


Figure 1: Rabi Oscillations

2 Lecture 2

In Lecture 1 we derived from first principals QM the probability of a transition from state 1 to 2 under a driving EM field. This was:

$$|c_2|^2 = \frac{|\Omega|^2}{W^2} \sin^2 \left(\frac{Wt}{2} \right) \quad (10)$$

$$W = \sqrt{|\Omega|^2 + (\omega - \omega_0)^2} \quad (11)$$

With the Rabi Frequency defined:

$$\Omega = \frac{\langle 1 | e\vec{r} \cdot \vec{E}_0 | 2 \rangle}{\hbar} = \frac{e}{\hbar} \int \psi_1 \vec{r} \cdot \vec{E}_0 \psi_2 d^3 r \quad (12)$$

Usually in problems, we assume the electric field along z and the vector \vec{E}_0 a constant. This results in us solving for the expectation of the electric dipole:

$$d = \langle \psi_1 | -ez | \psi_2 \rangle \quad (13)$$

If this expectation is zero, $|\Omega|^2 = 0$ and no transition is driven. Symmetry is used to quickly identify when $d = 0$.

2.1 Symmetry arguments

For $d = 0$ we require a matrix element of the sort:

$$\langle \psi_1 | -ez | \psi_2 \rangle = \langle \text{even} | \text{odd} | \text{even} \rangle \quad (14)$$

or

$$\langle \psi_1 | -ez | \psi_2 \rangle = \langle \text{odd} | \text{odd} | \text{odd} \rangle \quad (15)$$

In each case, the parity of the integral is odd, yielding a zero matrix element.

We obtain the parity of a wavefunction through rewriting the integral in spherical polars and sending $x, y, z \rightarrow -x, -y, -z$. Each transformation is equivalent to:

$$\mathbf{x} \rightarrow -\mathbf{x} \quad (16)$$

$$r \rightarrow r \quad (17)$$

$$\phi \rightarrow \pi - \phi \quad (18)$$

$$\theta \rightarrow \theta \quad (19)$$

$$\mathbf{y} \rightarrow -\mathbf{y} \quad (20)$$

$$r \rightarrow r \quad (21)$$

$$\phi \rightarrow -\phi \quad (22)$$

$$\theta \rightarrow \theta \quad (23)$$

$$\mathbf{z} \rightarrow -\mathbf{z} \quad (24)$$

$$r \rightarrow r \quad (25)$$

$$\phi \rightarrow \phi \quad (26)$$

$$\theta \rightarrow \pi - \theta \quad (27)$$

2.2 Hydrogen Transitions

We must satisfy the selection rules: $\Delta l = \pm 1$, $\Delta m = 0$ for linearly polarized light along z and $\Delta m = \pm 1$ for circularly polarized light in (x, y) .

Recall the relevant hydrogen atom wavefunctions for a transition driven from the ground state:

$$\psi_{100} = \psi_{1s0} = \frac{a_0^{-3/2}}{\sqrt{\pi}} \exp(-r/a_0) \quad (28)$$

$$\psi_{210} = \psi_{2p0} = \frac{a_0^{-3/2}}{4\sqrt{\pi}} \left[2 - \frac{r}{a_0} \right] \cos(\theta) \quad (29)$$

$$\psi_{21\pm 1} = \psi_{2p\pm 1} = \mp \frac{a_0^{-3/2}}{8\sqrt{\pi}} \frac{r}{a_0} \exp(-r/2a_0) \sin(\theta) \exp(\pm i\phi) \quad (30)$$

The transition from $1s0$ to $2p0$ is driven by linearly polarized light in the z direction. The wavefunction is a time dependent superposition of 2 states:

$$\Psi(\vec{r}, t) = c_1(t)\psi_{1s0} \exp(-iE_{1s0}t/\hbar) + c_2(t)\psi_{2p0} \exp(-iE_{2p0}t/\hbar) \quad (31)$$

Assuming $c_1(t) = c_2(t) = \frac{1}{\sqrt{2}}$:

$$\Psi(\vec{r}, t) = \frac{1}{\sqrt{2}} \exp(-iE_{1s0}t/\hbar) [\psi_{1s0} + \psi_{2p0} \exp(-i\omega_{12}t)] \quad (32)$$

$$\omega_{12} = \frac{E_{2p0} - E_{1s0}}{\hbar} \quad (33)$$

We can consider the relative phase term at different times and plot the probability distributions. The charge distribution is found to oscillate in the z axis.

Circularly polarized light in the (x, y) plane drives the $1s0$ to $2p1$ and $1s0$ to $2p-1$ transitions. Right circularly polarized light drives to $2p1$ and left to $2p-1$. The probability distributions of charge rotates clockwise and anticlockwise when viewed down the z axis respectively.

Be aware that if we viewed these transitions down the y or x axis, the emitted/absorbed light would appear linearly polarized.

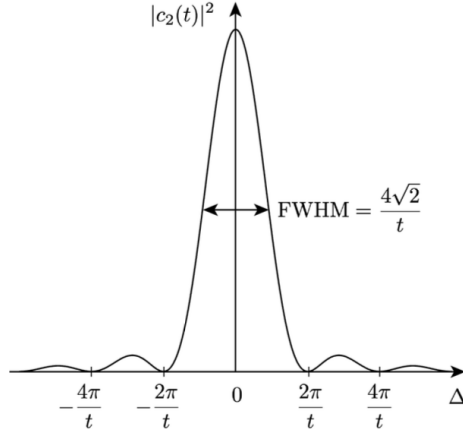


Figure 2: The transition probability as a function of Δ

3 Lecture 3

3.1 The Fractional Uncertainty of Atomic Clocks

The uncertainty of an atomic clock takes this form:

$$\sigma = \frac{\Delta\omega}{\omega} \sqrt{\frac{\tau_c}{N\tau}} \quad (34)$$

Here, the first part quantifies the uncertainty in the frequency of the atomic clock and the second part quantifies the uncertainty introduced by the limited number of measurements. τ_c is the time for one measurement, τ is the total integration time and N is the number of atoms tested.

We often break the structure down:

$$\frac{1}{Q} \left(\frac{1}{S/N} \right) \sqrt{\frac{1}{\tau}} \quad (35)$$

Where Q is the quality factor. In what follows we will look at methods to reduce $\Delta\omega$.

3.2 Transit Time Broadening

Recall the probability of being in state 2:

$$|c_2|^2 = \frac{|\Omega|^2}{W^2} \sin^2 \left(\frac{Wt}{2} \right) \quad (36)$$

$$W = \sqrt{|\Omega|^2 + (\omega - \omega_0)^2} \quad (37)$$

In the limit of a weak perturbation we obtain a sinc^2 function in Δ , Figure (2).

$$|c_2|^2 = \lim_{\Delta \gg \Omega} \frac{|\Omega|^2}{\Omega^2 + \Delta^2} \sin^2 \left(\frac{(\Omega^2 + \Delta^2)^{1/2} t}{2} \right) = \frac{|\Omega|^2}{\Delta^2} \sin^2 \left(\frac{\Delta t}{2} \right) = \frac{\Omega^2 t^2}{4} \text{sinc}^2 \left(\frac{\Delta t}{2} \right) \quad (38)$$

The width of the curve in Figure (2) defines the range of frequencies over which we can excite a significant transition. To quantify the width of the curve, we use an approximation of its FWHM:

$$\Delta\omega_{tt} = \frac{4\sqrt{2}}{t} \quad (39)$$

We would like this to be as small as possible. Hence we increase the **transit time**, t .

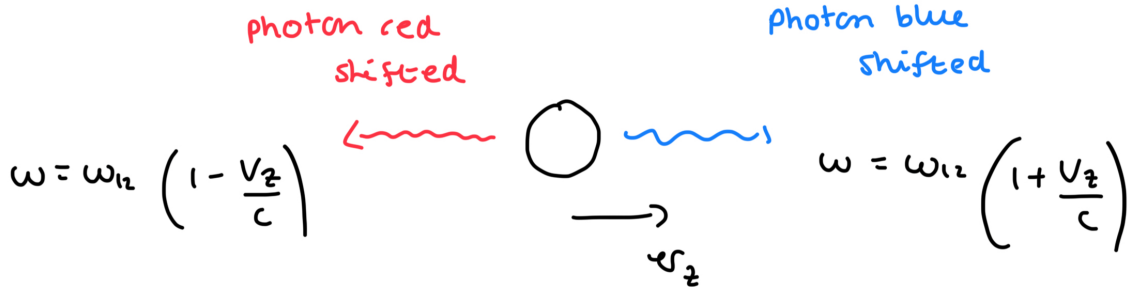


Figure 3: Doppler shift of photons for atoms

3.3 Doppler Broadening

Doppler Broadening arises due to the thermal motion of atoms. This implies there is a relative motion between the atom and the observer. The atom and the observer therefore view different frequencies due to the Doppler Shift. The quantity of the shift depends on the component of the atom's velocity along that of the photon's, Figure (3).

The Equations in Figure (3) are a low velocity binomial expansion of the relativistic Doppler equation. For red shift the equation is as follows

$$\omega_{obs} = \omega_{emit} \sqrt{\frac{1 - v/c}{1 + v/c}} \quad (40)$$

$$\omega_{obs} = \omega_{emit} \left(1 - \frac{v}{2c}\right) \left(1 - \frac{v}{2c}\right) \quad (41)$$

$$\omega_{obs} = \omega_{emit} \left(1 - \frac{v}{c}\right) \quad (42)$$

where the sign of v is flipped for the blue shift.

To describe the broadening we use the Maxwell Boltzmann Distribution. From Statistical Physics we have

$$P(E) \propto \exp\left(-\frac{E}{k_B T}\right) \quad (43)$$

$$E = \frac{1}{2}mv^2 \quad (44)$$

$$P(E) \propto \exp\left(-\frac{mv^2}{2k_B T}\right) \quad (45)$$

Normalization of the third expression gives:

$$P(v_z)dv_z = \left(\frac{m}{2\pi k_B T}\right)^{1/2} \exp\left(-\frac{mv_z^2}{2k_B T}\right) dv_z \quad (46)$$

A change of variable to frequency through Equation (42) gives:

$$P(\omega)d\omega = \frac{c}{\omega_{12}} \left(\frac{m}{2\pi k_B T}\right)^{1/2} \exp\left(-\frac{mc^2}{2k_B T} \frac{(\omega_{12} - \omega)^2}{\omega_{12}^2}\right) d\omega \quad (47)$$

This is a Gaussian and has a FWHM:

$$\Delta\omega_D = \frac{2\omega_{12}}{c} \left[\frac{2k_B T}{M} \ln(2) \right]^{1/2} \quad (48)$$

$$\Delta\omega_D = (7.16 \times 10^{-7}) \omega_{12} \left[\frac{T}{M_A} \right] \quad (49)$$

where M_A is the mass of the atom in **atomic units**.

3.4 Natural (Radiative) Broadening

Quantum Field Theory predicts the spontaneous decay of atoms from their excited states. The transition is induced by an interaction with the vacuum field. The rate of spontaneous emission is calculated through the Einstein A coefficient:

$$A_{21} = \frac{d^2\omega_{12}^2}{3\pi\epsilon_0\hbar c^3} \left(\frac{g_1}{g_2} \right) \quad (50)$$

Recalling that

$$\langle d \rangle^2 = |\langle 1| - ez|2\rangle|^2 \quad (51)$$

The lifetime of the excited state is:

$$\tau = \frac{1}{\Gamma} = \frac{1}{A_{21}} \quad (52)$$

From this we can describe the change in the population of the excited state due to spontaneous emission.

$$\frac{dN_2}{dt} = -A_{21}N_2 \implies N_2(t) = N_2(0)e^{-A_{21}t} \quad (53)$$

We now address why spontaneous decay causes broadening. The decay implies that

$$|c_2|^2 = e^{-\Gamma t} \implies c_2 = e^{-\Gamma t/2} \quad (54)$$

Then we have from lecture 1 that the classical evolution of the c_1 coefficient is:

$$i\dot{c}_1(t) = \frac{\Omega}{2} \exp(i(\omega - \omega_0)t) c_2 \quad (55)$$

We can substitute the exponentially decaying formula for $|c_2|$ to this and integrate between 0 and some time t . In the long time limit we obtain the formula:

$$|c_1|^2 = \frac{\Omega^2/4}{\Delta^2 + \Gamma^2/4} \quad (56)$$

The above equation implies a Lorenzian shape of $|c_1|^2$ with a FWHM $1/\Gamma$. This is the natural linewidth:

$$\Delta\omega_{nat} = \frac{1}{A_{21}} \quad (57)$$

It should be noted that the above logic is slightly heuristic as Rabi Oscillations and Spontaneous Emission aren't derived in the same physics frameworks.

3.5 The strength of Magnetic and Electric transitions

On average the electric dipole created in an atom has size $\sim ea_0$. We can consider the dipole created by the electron's magnetic moment. From CMP:

$$\vec{\mu} = -\frac{\mu_B}{\hbar} \vec{l} \quad (58)$$

We can then take a ratio of magnetic and electric dipole interactions:

$$|\frac{\vec{\mu} \cdot \vec{B}}{d \cdot \vec{E}}| = \frac{eL}{2m_e c} \frac{E}{ea_0 E} = \frac{\alpha}{2} = \frac{1}{274} \quad (59)$$

Recalling that the rate is $\propto d^2$ we have that electric dipoles have a natural broadening $\sim 10^5$ times larger. We therefore prefer to drive **magnetic transitions**. We have a smaller d and (usually) a smaller ω_{12} , reducing A_{21} .

4 Lecture 4

4.1 The Stern Gerlach Experiment

We can relate magnetic moments to angular momentum through Bohr Theory. Consider an electron orbiting the nucleus in a circle. We have that the electron sweeps out an area πr^2 . We can describe its current as $I = -ev/2\pi r$ and hence obtain a magnetic moment:

$$\vec{\mu}_l = -\frac{\mu_B}{\hbar} \vec{l} \implies \mu_{l,z} = -\frac{\mu_B}{\hbar} L_z = -\frac{\mu_B}{\hbar} m_l \hbar = -\mu_B m_l \quad (60)$$

Now, considering a hydrogen atom in a non-uniform magnetic field $(0, 0, B_z)$, the energy of the magnetic moment associated with orbital angular momentum is:

$$V = -\mu_{l,z} B_z = \mu_B m_l B_z \quad (61)$$

and the force on a beam of atoms must of atoms must be:

$$F_z = -\frac{d}{dz} \mu_B B m_l \quad (62)$$

If $m_l = 0$ we expect no force. However, the beam splits in 2 in the $l = 0$ state. Hence we are forced to conclude there is another magnetic moment in the electron. We associate this second magnetic moment with spin. Without proof we assume

$$\vec{\mu}_s = -g_s \frac{e}{2m_e} \vec{S} = -g_s \frac{\mu_B}{\hbar} \vec{S} \quad (63)$$

Now again, considering the potential in this non uniform magnetic field:

$$V = -\mu_{s,z} B_z = g_s \frac{e}{2m_e} m_s \hbar B_z = g_s \mu_B m_s B_z \quad (64)$$

implying

$$F = -\frac{d}{dz} g_s \mu_B m_s B_z \quad (65)$$

If the beam splits in 2, we have 2 different values for m_s . These correspond to spin-up and spin-down. Nuclei also have spin. The magnetic moments associated with electronic and nuclear spin are:

$$\begin{aligned} \vec{\mu}_s &= -g_s \mu_B \vec{S} & \vec{\mu}_I &= g_I \mu_N \vec{I} \\ \mu_B &= \frac{e}{2m_e} & \mu_N &= \frac{e}{2m_p} \\ g_s &\approx 2 & g_s &\approx 5.56 \end{aligned} \quad (66)$$

Here we have set $\hbar = 1$ (natural units).

It can therefore be assumed that different spin configurations can lead to different energy levels in an atom.

4.2 The Spin Orbit Interaction

In the electron's POV the proton moves in orbit about it, and creates a magnetic field. The magnetic moment associated with the electron's spin causes a perturbation in energy:

$$H' = -\vec{\mu}_s \cdot \vec{B} = A_{nl} \vec{S} \cdot \vec{L} \quad (67)$$

To compute the term $\vec{S} \cdot \vec{L}$ we consider:

$$\langle J^2 \rangle = \langle (L + S)^2 \rangle = \langle L^2 \rangle + \langle S^2 \rangle + \langle 2L \cdot S \rangle \implies L \cdot S = \frac{1}{2} [j(j+1) - l(l+1) - s(s+1)] \quad (68)$$

and hence:

$$H' = A_{nl} L \cdot S = \frac{A_{nl}}{2} [j(j+1) - l(l+1) - s(s+1)] \quad (69)$$

In perturbation theory, this is equivalent to finding eigen states of the operators H_0 , L^2 , J^2 , S^2 and J_z .

4.3 Hyperfine Structure

Fine structure (caused by the spin orbit interaction) is due to the electron seeing a magnetic field due to its own **orbital** angular momentum. Hyperfine structure is caused by the proton sitting in the magnetic field produced by the electron's total magnetic moment. This moment is due to the electron's spin and orbital angular momentum. The Hamiltonian takes the form:

$$H' = A_J \hat{I} \cdot \hat{J} \quad (70)$$

To obtain the eigen energies of H' we can again use:

$$\langle F^2 \rangle = \langle (I + J)^2 \rangle = \langle I^2 \rangle + \langle J^2 \rangle + \langle 2I \cdot J \rangle \implies I \cdot J = \frac{1}{2} [F(F+1) - I(I+1) - J(J+1)] \quad (71)$$

and

$$H' = A_J I \cdot J = \frac{A_J}{2} [F(F+1) - I(I+1) - J(J+1)] \quad (72)$$

In perturbation theory, this is equivalent to picking quantum numbers n, l, j, I, F, m_f .

4.4 Atomic Labeling

We define atomic states as follows:

$$n^{2s+1} L_J \quad (73)$$

5 Lecture 5

5.1 The Zeeman Effect

Placing an atom in an external magnetic field can shift the frequency of the clock transition, making our measurements inaccurate. We would like to identify states which are "Zeeman insensitive".

Consider the hydrogen atom in its ground state ($n = 0$ and hence $l = 0$). We shift the energy levels due to 2 effects: hyperfine splitting and the Zeeman effect. Fine structure is not relevant since it is in the ground state.

We can describe the perturbation:

$$H' = A_J \hat{I} \cdot \hat{J} - (\vec{\mu}_I + \vec{\mu}_J) \cdot \vec{B} \quad (74)$$

We can replace \vec{J} with \vec{S} since the atom is in its ground state. We can also neglect $\vec{\mu}_I$ since $m_p \gg m_e \implies \vec{\mu}_I \ll \vec{\mu}_s$. This gives:

$$H' = A_J \hat{I} \cdot \hat{S} - \vec{\mu}_S \cdot \vec{B} = A_J \hat{I} \cdot \hat{S} - g_s \mu_B B \hat{S}_z \quad (75)$$

5.2 Solving the Hamiltonian

The operators $\hat{I} \cdot \hat{S}$ and \hat{S}_z do not commute and therefore do not share a basis of eigenvectors. The eigenstates of $\hat{I} \cdot \hat{S}$ are expressed in terms of the quantum numbers $|F, m_F\rangle$. Those of \hat{S}_z are described by the quantum number m_s . We will express the eigenfunctions of $|F, m_F\rangle$ in terms of $|m_I, m_s\rangle$. Note we include m_I here even though its contribution to the Zeeman term has been set to zero.

To begin, we will define the $|m_I, m_s\rangle$ basis vectors. We consider the tensor product:

$$\begin{bmatrix} \alpha(1) \\ \beta(1) \end{bmatrix} \otimes \begin{bmatrix} \alpha(2) \\ \beta(2) \end{bmatrix} \quad (76)$$

and define the unit vectors in 4D space to each spin configuration:

$$|\uparrow\uparrow\rangle = (1, 0, 0, 0)^T \quad (77)$$

$$|\uparrow\downarrow\rangle = (0, 1, 0, 0)^T \quad (78)$$

$$|\downarrow\uparrow\rangle = (0, 0, 1, 0)^T \quad (79)$$

$$|\downarrow\downarrow\rangle = (0, 0, 0, 1)^T \quad (80)$$

We then find the $|F, m_F\rangle$ eigenvectors with respect to the $|m_I, m_s\rangle$ basis.

The $\hat{I} \cdot \hat{S}$ operator takes the form

$$\hat{I} \cdot \hat{S} = \hat{I}_x \otimes \hat{S}_x + \hat{I}_y \otimes \hat{S}_y + \hat{I}_z \otimes \hat{S}_z \quad (81)$$

with each component defined:

$$\hat{I}_x = \hat{S}_x = \frac{1}{2} \begin{bmatrix} 0 & 1 \\ 1 & 0 \end{bmatrix} \quad \hat{I}_y = \hat{S}_y = \frac{1}{2} \begin{bmatrix} 0 & -i \\ i & 0 \end{bmatrix} \quad \hat{I}_z = \hat{S}_z = \frac{1}{2} \begin{bmatrix} 1 & 0 \\ 0 & -1 \end{bmatrix} \quad (82)$$

The tensor product is calculated and the operator $\hat{I} \cdot \hat{S}$ evaluated. Its eigenvalues are then found through the characteristic equation. They are:

$$\lambda_1 = \frac{A}{4} \quad (83)$$

$$\lambda_2 = -\frac{3A}{4} \quad (84)$$

The first is 3 fold degenerate (triplet state) and the second is non-degenerate (singlet state). The eigenvectors can then be found. They are:

$$\lambda = \begin{cases} \frac{A}{4} & |\uparrow\uparrow\rangle, |\downarrow\downarrow\rangle, \frac{1}{\sqrt{2}}(|\uparrow\downarrow\rangle + |\downarrow\uparrow\rangle) \\ -\frac{3A}{4} & \frac{1}{\sqrt{2}}(|\uparrow\downarrow\rangle - |\downarrow\uparrow\rangle) \end{cases} \quad (85)$$

The eigenstates corresponding to $A/4$ form the triplet, they carry $F = 1$ (this can be seen by setting $I = J = 1/2$ in Equation (72)) with m_F defined as in standard QM. The eigenstate corresponding to $-3A/4$ has quantum numbers $F = 0$ and $m_F = 0$.

6 Lecture 6

6.1 Converting the Basis:

Previously, we found the eigenstates of the operator $\hat{I} \cdot \hat{S}$ with respect to the $|m_I, m_s\rangle$ basis. Now, let us switch the basis, we'd like to find the energy splitting with respect to the $|F, m_F\rangle$ basis.

Let us define new basis vectors:

$$|F = 1, m_f = 1\rangle = (1, 0, 0, 0)^T \quad (86)$$

$$|F = 1, m_f = 0\rangle = (0, 1, 0, 0)^T \quad (87)$$

$$|F = 0, m_f = 0\rangle = (0, 0, 1, 0)^T \quad (88)$$

$$|F = 1, m_f = -1\rangle = (0, 0, 0, 1)^T \quad (89)$$

$\hat{I} \cdot \hat{S}$ with respect to this basis must be:

$$\hat{I} \cdot \hat{S} = \begin{bmatrix} \frac{A}{4} & 0 & 0 & 0 \\ 0 & \frac{A}{4} & 0 & 0 \\ 0 & 0 & -\frac{3A}{4} & 0 \\ 0 & 0 & 0 & \frac{A}{4} \end{bmatrix} \quad (90)$$

Now we must evaluate the contribution from the $-g_s \mu_B B \hat{S}_z$ component. For this, we will convert the \hat{S}_z operator from the $|m_I, m_s\rangle$ basis to the $|F, m_F\rangle$ basis.

The matrix linking the two basis is defined through the eigenvectors of $|F, m_f\rangle$ with respect to the $|m_I, m_s\rangle$ basis:

$$|F, m_f\rangle = \begin{bmatrix} 1 & 0 & 0 & 0 \\ 0 & 1/\sqrt{2} & 1/\sqrt{2} & 0 \\ 0 & 1/\sqrt{2} & -1/\sqrt{2} & 0 \\ 0 & 0 & 0 & 1 \end{bmatrix} |m_I, m_s\rangle \quad (91)$$

From Linear Algebra I we have:

$$|F, m_f\rangle = \mathbf{U} |m_I, m_s\rangle \quad (92)$$

$$|m_I, m_s\rangle = \mathbf{U}^\dagger |F, m_f\rangle \quad (93)$$

Where \mathbf{U} is the matrix defined in Equation (89). We then also have the relationship:

$$\mathbf{D} = \mathbf{U} \mathbf{A} \mathbf{U}^\dagger \quad (94)$$

where \mathbf{U}^\dagger takes some input of states in the $|F, m_f\rangle$ basis and converts them to the $|m_I, m_s\rangle$ basis, \mathbf{A} is some operator defined with respect to the $|m_I, m_s\rangle$ basis. Then \mathbf{U} converts vectors in the $|m_I, m_s\rangle$ basis back to the $|F, m_f\rangle$ basis.

Hence, if we can find \hat{S}_z with respect to the $|m_I, m_s\rangle$ basis then we can find it with respect to the $|F, m_f\rangle$ basis.

The 4D \hat{S}_z matrix with respect to the $|m_I, m_s\rangle$ basis is:

$$\begin{bmatrix} 1 & 0 \\ 0 & 1 \end{bmatrix} \otimes \frac{1}{2} \begin{bmatrix} 1 & 0 \\ 0 & -1 \end{bmatrix} = \frac{1}{2} \begin{bmatrix} 1 & 0 & 0 & 0 \\ 0 & -1 & 0 & 0 \\ 0 & 0 & 1 & 0 \\ 0 & 0 & 0 & -1 \end{bmatrix} \quad (95)$$

We can then transform it to act in the $|F, m_f\rangle$ basis through

$$\hat{S}_z^{\{F, m_f\}} = \mathbf{U} \hat{S}_z^{\{m_I, m_s\}} \mathbf{U}^\dagger = \frac{1}{2} \begin{bmatrix} 1 & 0 & 0 & 0 \\ 0 & 0 & -1 & 0 \\ 0 & -1 & 0 & 0 \\ 0 & 0 & 0 & -1 \end{bmatrix} \quad (96)$$

We can multiply this matrix by $-g_s \mu_B B = -2\mu_B B$ and add it to that which describes $\hat{I} \cdot \hat{S}$ giving:

$$H' = \begin{bmatrix} \frac{A}{4} + \mu_B B & 0 & 0 & 0 \\ 0 & \frac{A}{4} & -\mu_B B & 0 \\ 0 & -\mu_B B & -\frac{3A}{4} & 0 \\ 0 & 0 & 0 & \frac{A}{4} - \mu_B B \end{bmatrix} \quad (97)$$

6.2 Solving the Hamiltonian

Again, we can solve the characteristic equation for the eigenvalues of energy with respect to the $|F, m_f\rangle$ basis. We obtain the following eigenvalues corresponding to $m_F = \pm 1$.

$$\lambda = \frac{A}{4} \pm \mu_B B = \frac{A}{2} \left(\frac{1}{2} \pm x \right) \quad (98)$$

where

$$x = \frac{2\mu_B B}{A} \quad (99)$$

similarly for $m_F = 0$ we obtain:

$$\lambda = -\frac{A}{4} \pm \frac{A}{2} (1 + x^2)^{1/2} \quad (100)$$

Note that these states are entangled in F . We can generalize through:

$$\lambda = -\frac{A}{4} \pm \frac{A}{2} (1 + 2mx + x^2)^{1/2} \quad (101)$$

where m is the magnetic quantum number. The above derivation was for hydrogen with a nuclear spin of $1/2$. For a single electron in an atom with nuclear spin I we have:

$$E = \pm \frac{A}{2} (1 + 2Mx + x^2)^{1/2} \quad (102)$$

$$M = \frac{2m_F}{2I + 1} \quad (103)$$

Here, we have shifted the energy origin by adding $A/4$.

6.3 Energy splitting under magnetic field

See Figure (4) for a break down of the hydrogen and cesium atom energy splitting. For hydrogen, note that:

- At zero magnetic field we have the exact energy splitting caused by the hyperfine interaction (shifted by $A/4$).
- As we increase the strength of the magnetic field, we obtain energies defined by Equation (101). The \pm in this equation refers to the upper and lower hyperfine states. At low B fields, the shifts are $\propto m_F$.
- The quantum states $|F, m_f\rangle$ are only appropriate for weak perturbation. If we increase the strength of the magnetic field, the hyperfine interaction becomes negligible and we use the $|m_I, m_s\rangle$ basis.

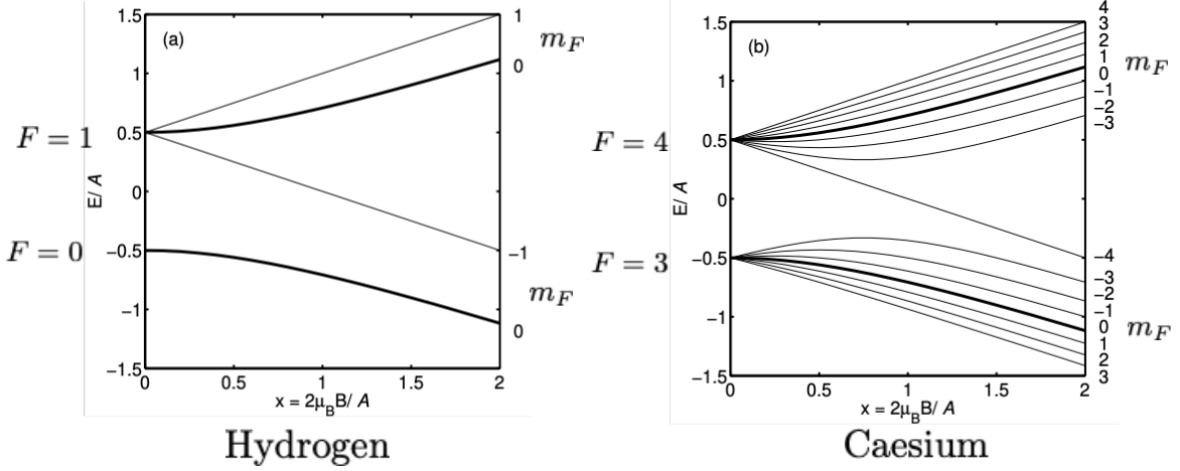


Figure 4: Zeeman Energy splitting at low magnetic field

When considering the high field (Paschen Bach) region, we have a Hamiltonian dominated by the Zeeman effect. We now account for the nuclear spin.

$$H_z = \mu_B \vec{B} \cdot \vec{S} + \mu_N \vec{B} \cdot \vec{I} \quad (104)$$

$$H_z = -[g_s \mu_B \vec{S} \cdot \vec{B} + g_I \mu_N \vec{I} \cdot \vec{B}] \quad (105)$$

$$H_z = g_s \mu_B \vec{S} \cdot \vec{B} - g_I \mu_N \vec{I} \cdot \vec{B} \quad (106)$$

The highest energy system is when the electron spin is aligned and the nuclear spin is anti-aligned, then when the electron spin is aligned and the nuclear aligned, then when the electron spin is anti-aligned and the nuclear spin is anti-aligned, and finally when the electron spin is anti-aligned and the nuclear spin is aligned. $|m_I, m_s\rangle$ becomes the relevant basis.

6.4 The Zeeman Shift

We define the transition frequency between a lower and upper hyperfine state as:

$$\gamma(x) = [E_{F',m'_F} - E_{F,m_F}] / h \quad (107)$$

$$\gamma(x) = \frac{A}{2h} [(1 + 2M'x + x^2)^{1/2} + (1 + 2Mx + x^2)^{1/2}] \quad (108)$$

The **Zeeman Shift** is defined as the change in transition frequency after a magnetic field is applied:

$$\Delta v = v(x) - v(0) \quad (109)$$

$$\Delta v = \frac{A}{2h} [(1 + 2M'x + x^2)^{1/2} + (1 + 2Mx + x^2)^{1/2} - 2] \quad (110)$$

Considering a weak magnetic field, we expand to 1st order:

$$\Delta v = \frac{A}{2h} [(M' + M)x] \quad (111)$$

Importantly, for an atomic clock we want to minimize the Zeeman Shift on the clock transition, hence we use $M = M' = 0$ and to first order have $\Delta v = 0$. We call this the **magnetically insensitive transition**.

There are further selection rules for F :

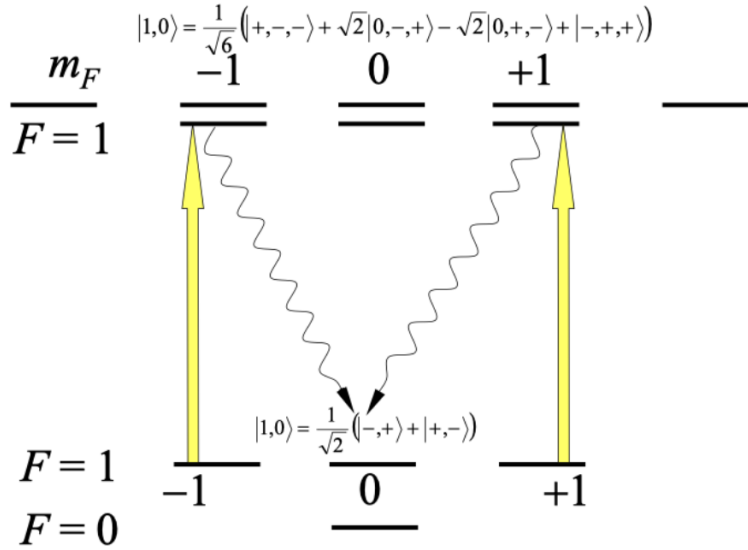


Figure 5: Optical Pumping

- $\Delta F = 0, \pm 1, \Delta m_F = 0, \pm 1$
- No transition can be driven between $F = 0$ and $F' = 0$.
- No transition can be driven between $m_F = 0 \rightarrow m_{F'} = 0$ for $F = F'$.

The above selection rules are used to ensure the state $|F = 1, m_F = 0\rangle$ is populated and that the magnetically insensitive transition between $|F = 1, m_F = 0\rangle$ and $|F = 0, m_F = 0\rangle$ is driven. See Figure (5).

The Earth's magnetic field is $\sim 50 \mu\text{T}$, it is significant enough to cause a Zeeman shift, even of the magnetically insensitive state. We require magnetic shielding.

7 Lecture 7

7.1 The Stern Gerlach Experiment (again)

Consider a beam of atoms being fired through a magnetic field with variation in z . We can consider the force:

$$F_z = -\frac{dV}{dz} = -\frac{d}{dz} - \vec{\mu} \cdot \vec{B} = \frac{d}{dz} \mu_z B_z(z) = -g_s \gamma S_z \frac{d}{dz} B_z(z) = -g_s \gamma \hbar m_s \frac{dB_z(z)}{dz} = \mp \mu_B \frac{dB_z(z)}{dz} \quad (112)$$

Where we have defined the force for $m_s = +1/2$ and $m_s = -1/2$ respectively.

7.2 The Atomic beam clock

This works on a similar principal to the Stern Gerlach Experiment. See Figures (6) and (8). Here, we describe the "Flop in" arrangement. Consider the $m_J = +1/2$ beam. The force on this beam always opposes the direction of the magnetic gradient. It is pushed upward when the gradient points downward in region 1. In region 2, there is a low magnetic field and we drive the clock transition, aiming to flip the quantum state. When the beam comes out, it is (ideally) in $m_J = -1/2$ moving upward. The force on this beam is always in the same direction as the magnetic gradient. The beam is then forced downward and hits the detector.

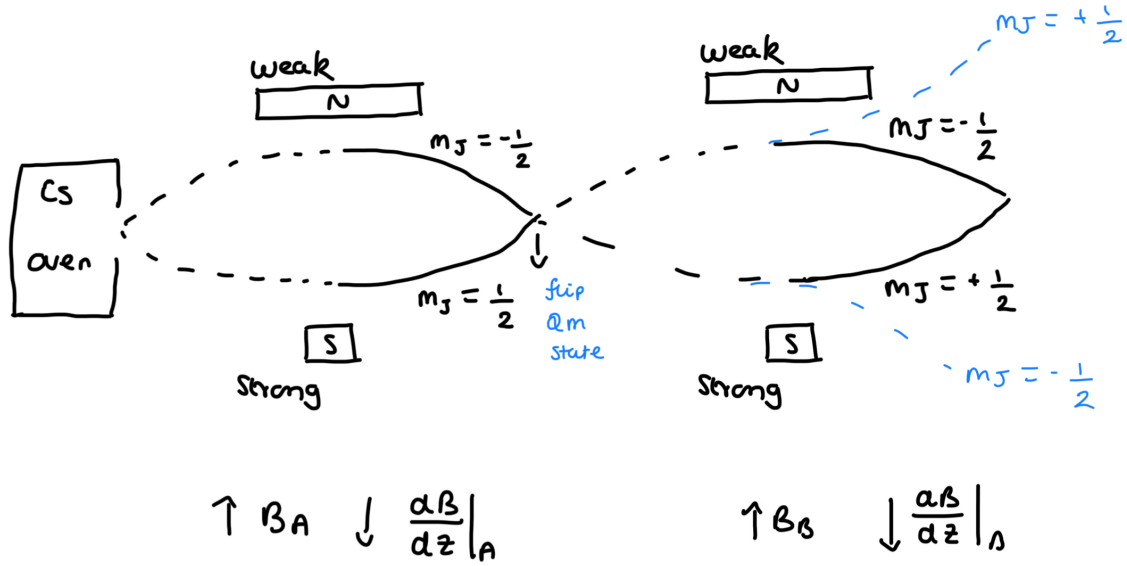


Figure 6: The Atomic Beam Clock in the 'Flop In' arrangement. The blue dashed lines show the trajectory of atoms which do not change their atomic states.

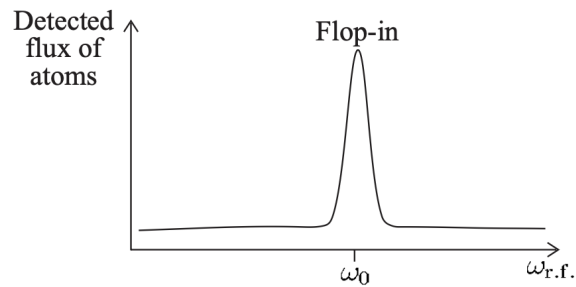


Figure 7: Flop in

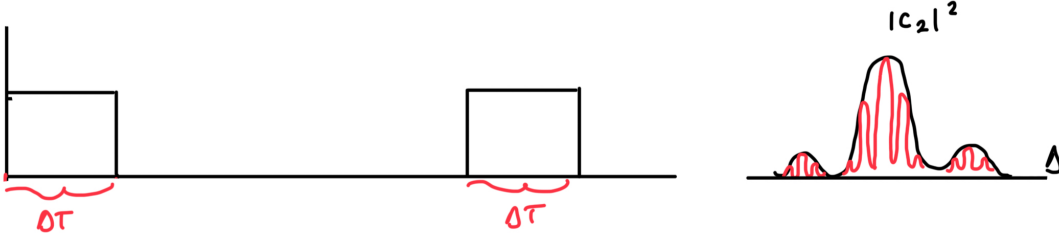


Figure 8: Ramsey Pulses and the resulting interferometry curve

If the clock transition is not driven at the right frequency, the flip in quantum state does not occur and the beam will not hit the detector. This is the dashed line in Figure (6).

Note that the initial population of the 2 hyperfine states is approximately the same since:

$$\frac{P_1}{P_2} \approx \exp\left(\frac{\hbar\omega_{21}}{k_B T}\right) \quad (113)$$

and $\hbar\omega_{21} \ll k_B T$.

7.3 The Ramsey Method

Consider the interaction region. The Rabi Method is to apply a constant excitation pulse over the whole region for a time $\tau = L_c/v$.

Recall that τ should be as large as possible to minimize transit time broadening. Hence, L_c should be very long. In practice it is challenging to apply a non-fluctuating magnetic field over a long region. Ramsey developed a solution.

He suggested altering the superposition of states through $2\pi/2$ pulses (lasting ΔT) with a free evolution in between (see Figure (8)). The $\pi/2$ pulses excite the system from the ground state to a 50-50 superposition, and to the excited state respectively. The maths requires an understanding of the Bloch Sphere and is too complex, but the result is significant.

The probability of the atom being found in the excited state $|c_2|^2$ is:

$$|c_2|^2 \propto \cos^2\left(\frac{\tau}{2}\right) \quad (114)$$

This is atomic interferometry. The plot of $|c_2|^2$ against Δ is now of \cos^2 fringes with a sinc^2 envelope. The FWHM of the curve is

$$\Delta\omega_{tt} = \frac{\pi}{\tau} \quad (115)$$

This results in higher precision than the Rabi Method, (where the FWHM is $\frac{4\sqrt{2}}{t}$) since $\tau \gg t$

8 Lecture 8

8.1 The Scattering Rate

Light forces arise because photons carry momentum. The absorption and emission of light exerts force on the atom. Recall that for a photon:

$$E = \hbar\omega = pc \quad (116)$$

Atoms receive a momentum 'kick' in the direction of absorption and in the opposite direction to emission. However, photons are emitted in random directions, so the net momentum kick on emission is zero.

We define the scattering rate (R_{scatt}) as the average number of photons scattered (absorbed and re-emitted) per atom per unit time. The average momentum transferred in 1 second (or continuous Force applied to the atom) is therefore

$$F = \frac{dp}{dt} = \hbar k R_{scatt} \quad (117)$$

The scattering rate itself is defined:

$$R_{scatt} = \Gamma |c_2|^2 \quad (118)$$

where Γ is the spontaneous emission rate (number of photons emitted per second when the atom is excited) and $|c_2|^2$ is the probability that the atom is excited.

8.2 Einstein's Treatment

In lecture 1 we derived a classical expression for $|c_2|^2$ under a coherent laser. This did not account for spontaneous emission. We will now derive an expression for $|c_2|^2$ for a system in thermal equilibrium with a photon gas (Blackbody radiation), which accounts for spontaneous emission.

In a blackbody gas, atom light interactions are governed by 3 processes:

1. Spontaneous emission, at a rate A_{21}
2. Absorption, at a rate $B_{12}\rho(\omega_{12})$
3. Stimulated emission, at a rate $B_{21}\rho(\omega_{12})$

where $\rho(\omega_{12})$ is the energy density per unit volume. Our first goal will be to define B. Let N_a be the number of atoms in the ground state ψ_a and let N_b be the number of atoms in the excited state ψ_b . In thermal equilibrium the number of atoms entering state B per second must equal the number of atoms leaving it. Hence:

$$N_b A_{21} + N_b B_{21}\rho(\omega_{12}) = N_a B_{12}\rho(\omega_{12}) \quad (119)$$

Since $B_{12} = B_{21}$ we have

$$\rho(\omega_{12}) = \frac{A}{B} \frac{1}{N_a/N_b - 1} \quad (120)$$

and we have independently derived the energy density per unit volume. From statistical mechanics we have:

$$\frac{N_a}{N_b} = \frac{g_a}{g_b} \exp\left(\frac{\hbar\omega_{12}}{k_B T}\right) \quad (121)$$

and hence, assuming $g_a = g_b$:

$$\rho(\omega_{12}) = \frac{A}{B} \frac{1}{\exp(\frac{\hbar\omega_{12}}{k_B T}) - 1} = \frac{\hbar\omega_{12}^3}{\pi^2 c^3} \frac{1}{\exp(\frac{\hbar\omega_{12}}{k_B T}) - 1} \quad (122)$$

Using the expression for A_{21} from lecture 1, we can define B :

$$B = \frac{\pi d^2}{3x\epsilon_0\hbar^2} \quad (123)$$

We are then in a position to calculate dN_2/dt , N_2 and therefore $|c_2|^2$.

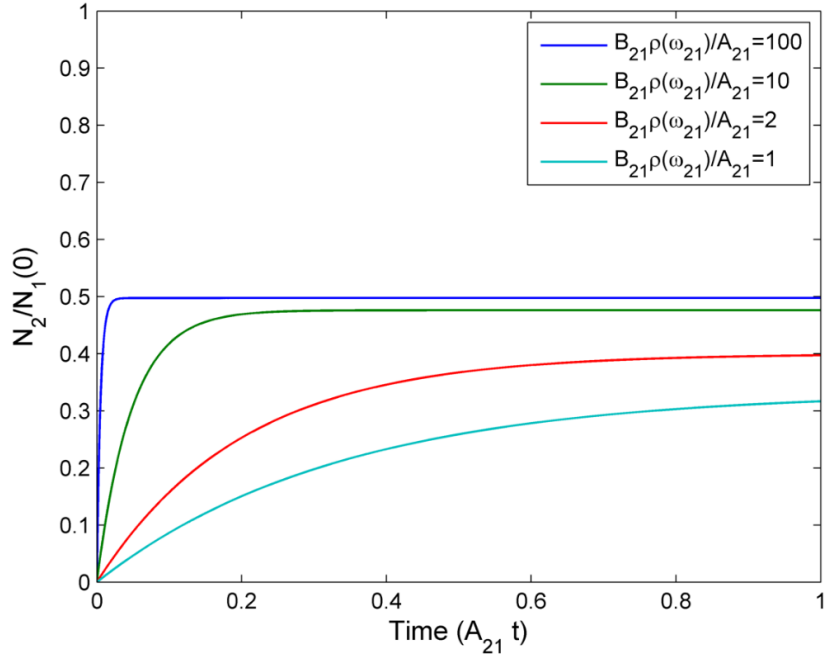


Figure 9: $|c_2|^2$ against time, derived using Einstein's treatment of an atom in Blackbody radiation.

8.3 $|c_2|^2$ from Einstein's Treatment

We will start by defining the rate of change of N_2 . Let N be the total number of atoms in the system. We have:

$$\frac{dN_2}{dt} = B_{12}\rho(\omega_{12})(N - N_2) - N_2B_{21}\rho(\omega_{21}) - N_2A \quad (124)$$

$$\frac{dN_2}{dt} = B_{12}N\rho(\omega_{12}) - N_2[A + 2B_{12}\rho(\omega_{12})] \quad (125)$$

$$\frac{dN_2}{dt} + [A + 2B_{12}\rho(\omega_{12})]N_2 = B_{12}N\rho(\omega_{12}) \quad (126)$$

This is a first order homogeneous differential equation. The solution is as follows:

$$\frac{N_2}{N} = \frac{B\rho(\omega_{12})}{A + 2B\rho(\omega_{12})}[1 - \exp(-[A + 2B\rho(\omega_{12})]t)] \quad (127)$$

It can be seen that as $t \rightarrow \infty$ the second term tends to 1 and N_2/N converges to the primary factor.

See Figure (9). The larger the ratio of $B\rho(\omega_{12})/A_{21}$ the larger the value the curve converges to and the faster the curve converges. The dark blue line shows a convergence to a constant 50-50 superposition state.

9 Lecture 9

In this lecture, we build on our study of the interaction between monochromatic, coherent light and a two-level atomic system. Specifically, we aim to model how the intensity of such light evolves as it propagates through a medium containing many atoms.

9.1 Modeling an Incoherent Two-Level System

In Lecture 1, we modeled the two-level system using Rabi oscillations, assuming purely coherent, wave-like evolution. However, in realistic atomic systems, spontaneous emission leads to decoherence,

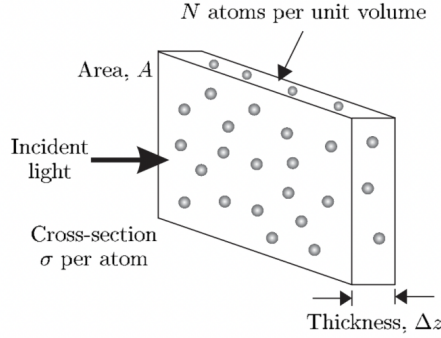


Figure 10: A layer of atoms interacting with laser radiation.

making the evolution stochastic rather than deterministic. As a result, we describe the system using the rate equations, which track the populations of each energy level over time, rather than the full quantum state.

We recall Einstein's coefficients, which give the probability per unit time for atomic transitions. In Einstein's original treatment, transitions occur only at the exact frequency ω_{12} . However, in reality, broadening effects (discussed in Lecture 3) mean atoms can interact with a narrow range of nearby frequencies. To account for this, each coefficient is multiplied by a Lorentzian line shape $L(\omega)$.

$$L(\omega) = \frac{\Gamma/2\pi}{(\omega - \omega_{12})^2 + \Gamma^2/4} \quad (128)$$

The probability of stimulated emission/absorption and of spontaneous emission per unit time per unit frequency become:

$$b\rho(\omega_{12}) = B\rho(\omega_{12})L(\omega) \quad (129)$$

$$a_{21} = A_{21}L(\omega) \quad (130)$$

Each of these is a probability density function in time and frequency space. For example $b_{12}\rho(\omega_{12})dt d\omega$ gives the probability that a single atom will undergo a transition in the time interval dt due to radiation in a frequency range $[\omega, \omega + d\omega]$.

9.2 The Absorption Cross-section

Considered a weak beam of light with a narrow band width $d\omega$ passing a cloud of atoms, Figure (10). We make two assumptions when modeling the intensity change of the beam:

- The atoms have reached the steady state, such that the populations of the energy states do not change in time.
- Spontaneous emission is neglected. This is justified as the emission is isotropic and we are considering a laser beam.

Equating expressions for energy change of the beam per unit time:

$$[I(z + dz) - I(z)]Ad\omega = [N_2 B_{21}L(\omega)\rho(\omega_{12})d\omega - N_1 B_{12}L(\omega)\rho(\omega_{12})d\omega]\hbar\omega Adz \quad (131)$$

The LHS of this equation is the energy change of the beam per unit second due to radiation in a small frequency range $d\omega$. The first term on the RHS gives the energy added to the beam by stimulated emission: the transition rate per atom times the number of excited atoms ($N_2 Adz$) and the photon energy ($\hbar\omega$). The second term is the corresponding energy loss due to absorption by atoms in the ground state.

We can take the limit that $dz \rightarrow 0$ and substitute the relationships:

$$\rho(\omega_{12}) = \frac{I(\omega_{12})}{cd\omega} \quad (132)$$

$$g_1 B_{12} = g_2 B_{21} \quad (133)$$

$$B_{21} = \frac{A_{21}\pi^2 c^3}{\hbar\omega_{12}^2} \quad (134)$$

to obtain

$$\frac{1}{I} \frac{dI}{dz} = \frac{\pi^2 c^2}{\omega_{12}^2} A_{21} L(\omega) [N_2 - \frac{g_2}{g_1} N_1] \quad (135)$$

The component in red is the absorption cross section:

$$\sigma(\omega) = \frac{\pi^2 c^2}{\omega_{12}^2} A_{21} L(\omega) \quad (136)$$

At resonance ($\omega = \omega_{12}$) we can replace $L(\omega)$ with $\frac{2}{\pi\Gamma}$ and approximate $\pi \sim 3!$ This gives

$$\sigma(\omega_{12}) = \frac{3\lambda^2}{2\pi} = \frac{\lambda^2}{2} \quad (137)$$

9.3 The Intensity Profile

The intensity equation above is a first order homogeneous differential equation. Calling the RHS of the equation $k(\omega)$, the solution is:

$$I = I(\omega, z = 0) \exp(-k(\omega)z) \quad (138)$$

This is the Beer-Lambert Law, where intensity shows an exponential decay. Note that the rate of exponential decay is not necessarily constant. It depends on the absorption cross-section and the relative occupation of ground and excited states. Assuming $g_1 = g_2$ for simplicity:

$$k(\omega) = \sigma(\omega)[N - 2N_2] \quad (139)$$

We will now investigate how the intensity of radiation alters the relative population of the states.

9.4 Saturation

We now study the steady state of a laser beam passing through a material. We consider an energy balance, including spontaneous emission:

$$(N_1 - N_2)\sigma(\omega)I = N_2 A_{21} \hbar\omega \quad (140)$$

Defining the ratio

$$r^{-1} = \frac{\sigma(\omega)I}{A_{21} \hbar\omega} \quad (141)$$

and using the condition that $N = N_1 + N_2$ we obtain:

$$N_1 - N_2 = \frac{N}{1 + 2r^{-1}} = \frac{N}{1 + I/I_s} \quad (142)$$

where I_s is defined

$$I_s(\omega) = \frac{A_{21} \hbar\omega}{2\sigma(\omega)} \quad (143)$$

If $I = I_s$ it can be shown that $N_2 \rightarrow \frac{N}{4}$ which implies the absorption coefficient $k(\omega)$

$$\frac{k(I_s)}{k(I)_{max}} = \frac{\sigma(\omega)}{\sigma(\omega)} \frac{N/2}{N} = 1/2 \quad (144)$$

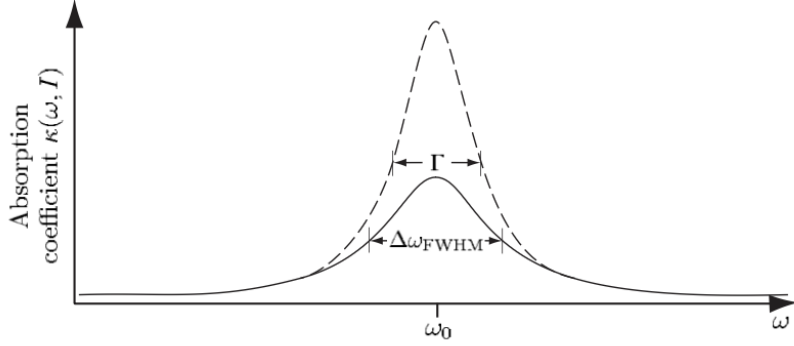


Figure 11: Power Broadening

has decreased to half its maximum value.

When $I \ll I_s$ $k(\omega, I) \sim \sigma(\omega)N \rightarrow$ strong absorption, and when $I \gg I_s$ $k(\omega, I) \sim \sigma(\omega)NI_s(\omega)/I \rightarrow$ weaker absorption.

The minimum value of I_s is at resonance, this is called I_{sat} .

$$I_{sat}(\omega) = \frac{A_{21}\hbar\omega}{2\sigma(\omega_{12})} = \frac{A_{21}\hbar\omega}{2} \frac{2\pi}{3\lambda^2} = \frac{\pi hc}{3\lambda^3\Gamma} \quad (145)$$

9.5 The absorption coefficient $k(\omega, I)$

We can rewrite the absorption coefficient to show its explicit frequency dependence. Combining Equations (137) and (140) gives:

$$k(\omega, I) = \sigma(\omega)N \frac{1}{1 + \frac{I}{I_{sat}(\omega)}} \quad (146)$$

Each $\sigma(\omega)$ and $I(\omega)$ can be manipulated to obtain this form of the absorption coefficient (see Appendix 1):

$$k(\omega, I) = \frac{N\sigma(\omega_{12})\Gamma^2/4}{(\omega - \omega_{12})^2 + \Gamma^2/4} \times \frac{1}{1 + \frac{I}{I_{sat}} \left(\frac{\Gamma^2/4}{(\omega - \omega_{12})^2 + \Gamma^2/4} \right)} \quad (147)$$

This formula demonstrates the explicit frequency and intensity dependence of the absorption coefficient. In frequency space k has a Lorentzian line shape with a FWHM:

$$\Delta\omega_{FWHM} = \Gamma(1 + I/I_{sat})^{1/2} \quad (148)$$

From this, we interpret that if we increase the intensity of radiation a significant absorption occurs over a larger range of frequencies, Figure (11). This is called **Power Broadening**.

9.6 The Spontaneous Scattering Force

Recall that we said the spontaneous scattering force was

$$F = \hbar k R_{scatt} = \hbar k \Gamma |c_2|^2 \quad (149)$$

We have developed expressions for $|c_2|^2$ under assumption of coherent laser light and incoherent black body radiation. The Optical Bloch Equations (not on syllabus) derive $|c_2|^2$ when the excitation is created by an **incoherent laser beam**. This gives the following scattering force:

$$F_{max} = \frac{\hbar k \Gamma}{2} \frac{\Omega^2/4}{\Delta^2 + \Omega^2/2 + \Gamma^2/4} \quad (150)$$

and the relation:

$$\frac{I}{I_{sat}} = \frac{2\Omega^2}{\Gamma^2} \quad (151)$$

Through substitution and algebra we obtain:

$$F_{max} = \frac{\hbar k \Gamma}{2} \frac{I}{I + I_{sat} \left[1 + \frac{4\Delta^2}{\Gamma^2} \right]} \quad (152)$$

10 Lecture 10

So far we have studied atomic beam clocks, where the uncertainty is dominated by transit time broadening. To reduce this contribution to the uncertainty, we would like to confine the atoms and take longer measurements.

10.1 The Principals of Confinement

Confinement starts with reducing the velocity of atoms, which can be done by cooling them (recall the Boltzmann velocity distribution):

$$P(v_z) \propto \exp \left(\frac{mv_z^2}{2k_B T} \right) \quad (153)$$

We decelerate atoms using the spontaneous/scattering force. Consider an atom traveling in the $+z$ direction toward a laser beam with a frequency ω_l close to the atom's resonance.

The atom experiences a blue shifted frequency, ω_a :

$$\omega_a = \omega_l \left(1 + \frac{v_z}{c} \right) \quad (154)$$

For a maximum scattering force, Equation (151), we require $\Delta = \omega_a - \omega_{12} = 0 \implies \omega_a = \omega_{12}$. Hence we need $\omega_l < \omega_{12}$. The required $\omega_{12} - \omega_l$ is therefore:

$$\omega_{12} = \omega_l \left(1 + \frac{v_z}{c} \right) \implies \omega_{12} - \omega_l = \frac{\omega_l v_z}{c} = kv_z \quad (155)$$

Where v_z is the velocity of a atom in the lab frame and k is the wave vector of the laser in the lab frame.

However, as the beam slows down, the factor $(1 + v_z/c)$ reduces and the atoms come out of resonance with the laser beam. To compensate for this we can:

- Change the frequency of the radiation over time. This is called Chirp Cooling. The technique only works on pulses of atoms, as the change in laser frequency cannot be made instantaneously.
- Shift the resonant frequency in the atom with position using a magnetic field. This is **Zeeman Deceleration**

10.2 Zeeman Deceleration

To understand how to modify the frequency of the laser beam, we need to predict an atom's velocity profile under spontaneous scattering. Recalling the formula for the scattering force:

$$F_{scatt} = \frac{\hbar k \Gamma}{2} \frac{I/I_{sat}}{1 + I/I_{sat} + 4\Delta^2/\Gamma^2} \quad (156)$$

The maximum scattering force is therefore given by the pre-factor as $I \rightarrow \infty$ and the maximum acceleration of an atom of mass M is:

$$a_{max} = \frac{F_{max}}{M} = \frac{\hbar k \Gamma}{M} \frac{v_r}{2\tau} = \frac{v_r}{2\tau} \quad (157)$$

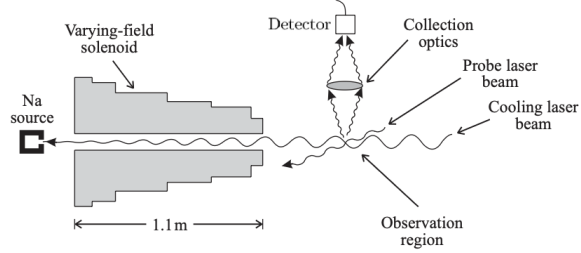


Figure 12: The first Zeeman Slower

where v_r is the recoil velocity. Usually, $a = a_{max}/2$ and the stopping distance given by $v^2 = v_0^2 + 2as$ is:

$$L_0 = \frac{v_0^2}{a_{max}} \quad (158)$$

All alkali metals have a similar L_0 values. To define the velocity profile of the atom, consider it's speed at some arbitrary position between $z = 0$ and $z = L_0$.

$$v^2 = v_0^2 + 2as \quad (159)$$

$$a = -\frac{v_0^2}{2L_0} \quad (160)$$

$$v^2 = v_0^2 - 2\frac{v_0^2}{2L_0}z \quad (161)$$

$$v = v_0 \left[1 - \frac{z}{L_0} \right]^{1/2} \quad (162)$$

Now recalling the Zeeman Shift in frequency given by Equation (110), and assuming $M' + M = 1$, for atomic resonance it is required that:

$$\omega_{12} + \frac{\mu_B B(z)}{\hbar} = \omega_l + kv_z \quad (163)$$

where the LHS represents the original transition frequency, shifted by the Zeeman effect, and the RHS is the frequency the atom experiences.

To obtain the velocity profile above we use a magnetic field with the following form:

$$B(z) = B_0 \left[1 - \frac{z}{L_0} \right]^{1/2} + B_{bias} \quad (164)$$

where B_{bias} is added so we can define some non-zero final velocity. Substituting Equations (160) and (162) into (161) we obtain an expression for B_0 :

$$B_0 = \frac{\hbar v_0}{\lambda \mu_B} \quad (165)$$

and if the atoms come to a complete stop it is required that

$$\mu_B B_{bias} = \hbar(\omega_l - \omega_{12}) \quad (166)$$

Zeeman decelerators are useful for **fast** atoms e.g. Li, which need heating to a high temperature to be atomized. See Figure (12).

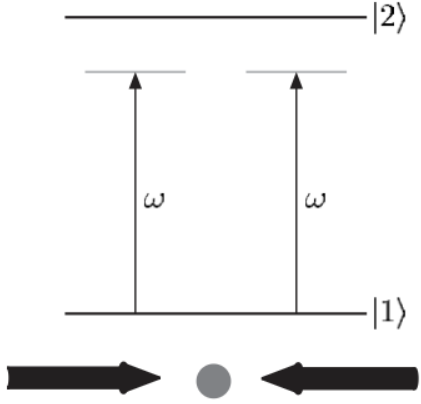


Figure 13: A stationary atom under 2 red de-tuned lasers

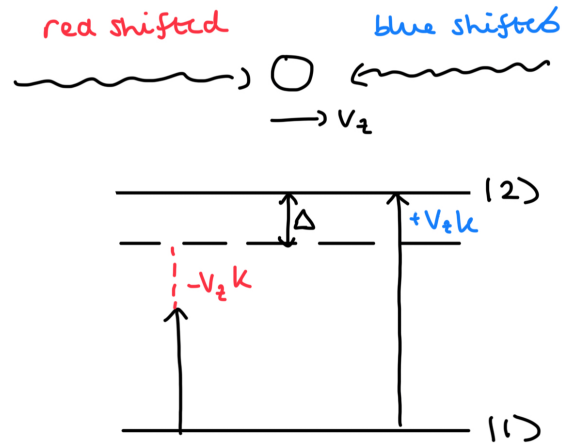


Figure 14: A moving atom under the 2 lasers

10.3 Optical Molasses

In the following $\Delta = \omega_a - \omega_{12}$.

Consider an atom in 2 counter propagating laser beams. If the atom is stationary and the laser beams are red de-tuned, a small scattering force is applied in each direction and the atom does not accelerate. Figure (13).

Now consider the scenario in which the atom moves, Figure (14). More light scatters from the beam which opposes the atom's motion. The atom experiences a different frequency from each laser beam. The frequency experienced by the **blue shifted beam is higher** and that experienced by the **red shifted beam is lower**:

$$\omega_a = \omega_L \left(1 \pm \frac{v_z}{c} \right) \quad (167)$$

$$\omega_a = \omega_L \pm v_z k \quad (168)$$

We can consider that the de-tuning $\Delta = \omega_a - \omega_{12}$ takes on different values for each beam (see Figure (14)):

$$\Delta' = \Delta \mp v_z k \quad (169)$$

The force due to each laser beam can then be defined:

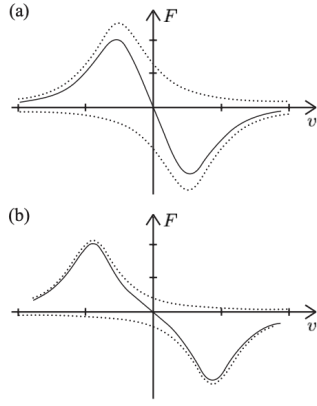


Figure 15: Force velocity profiles for de-tuning of $\Gamma/2$ in (a) and Γ in (b)

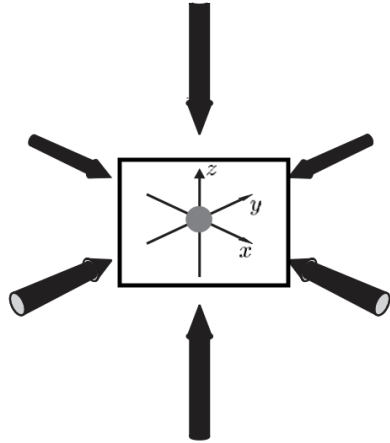


Figure 16: Optical Molasses

$$F_{\pm} = \frac{\pm \hbar k \Gamma}{2} \frac{I}{2I + I_{sat} \left[1 + 4 \left(\frac{\Delta \mp v_z k}{\Gamma} \right)^2 \right]} \quad (170)$$

The factor of 2 in front of I has been added to account for the fact that both beams contribute to saturation, the full reasoning is derived in the Optical Bloch Equations (not on syllabus).

The total force on the atom is $F = F_+ + F_-$. This gives the net force velocity profile depicted in Figure (15). We define the region between $\pm\Gamma/k$ the 'capture range' of the plot, where the net force is most significant.

The total force can be approximated in the small velocity limit ($kv_z < \Gamma$):

$$F_{\pm} = \hbar k \frac{2\Delta}{\Gamma} \frac{4kv_z}{\left(1 + \frac{4\Delta^2}{\Gamma^2} \right)} \quad (171)$$

From this it is clear that the atoms experience a force proportional to velocity, such as friction. $F = -\alpha v_z$.

Using three sets of beams along the cartesian axis, we get 3D cooling or **optical molasses**, Figure (16).

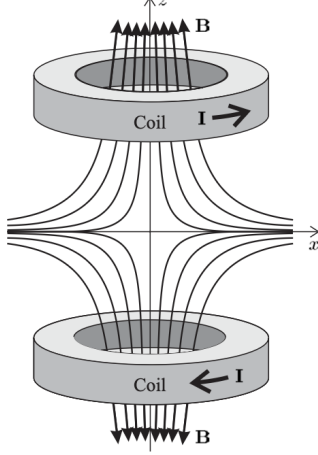


Figure 17: The quadrupole magnetic field

10.4 The Doppler Cooling Limit

The derivation is not required, but the minimum temperature of optical molasses is:

$$T_{min} = \frac{\hbar\Gamma}{2k_B} \frac{1 + (\frac{2\Delta}{\Gamma})^2}{-\frac{2\Delta}{\Gamma}} \quad (172)$$

This is a minimum for red de-tuned laser frequency at $\Delta = \omega_a - \omega_{12} = -\frac{\Gamma}{2}$. This is known as the Doppler limit:

$$T_D = \frac{\hbar\Gamma}{2k_B} \quad (173)$$

Equating the thermal and kinetic energies gives the most probable velocity v_D :

$$\frac{\hbar\Gamma}{2k_B} = \frac{1}{2}mv_D^2 \implies v_D = \left[\frac{\hbar\Gamma}{m} \right]^{1/2} \quad (174)$$

Sometimes we express v_D in terms of the recoil and capture velocities v_r and v_c respectively:

$$v_D = \left[\frac{\hbar k}{m} \frac{\Gamma}{k} \right]^{1/2} = [v_r v_c]^{1/2} \quad (175)$$

11 Lecture 11

In Lecture 10 we studies optical molasses. This is a method of deceleration. Now we need a way to **trap** the atoms once they have been cooled.

11.1 The Magneto-optical Trap

The Magneto-optical Trap (MOT) is comprised of 6 circularly polarized beams and a spatially varying magnetic field. The magnetic field introduces a strong Zeeman shift and causes an imbalance of the scattering forces from the laser beams. It is the scattering force which strongly confines the atoms.

We use a quadrupole magnetic field. This is created using 2 coils with currents in opposite directions. The field is zero at the origin and increases in magnitude in all directions. Figure (19).

The MOT is illustrated in Figure (18). Near the origin, the magnetic field is approximately uniform, and the Zeeman shift is described using the quantum states $|J, m_J\rangle$, as the magnetic field is relatively strong compared to hyperfine interactions. The field changes direction on either side of the origin, which

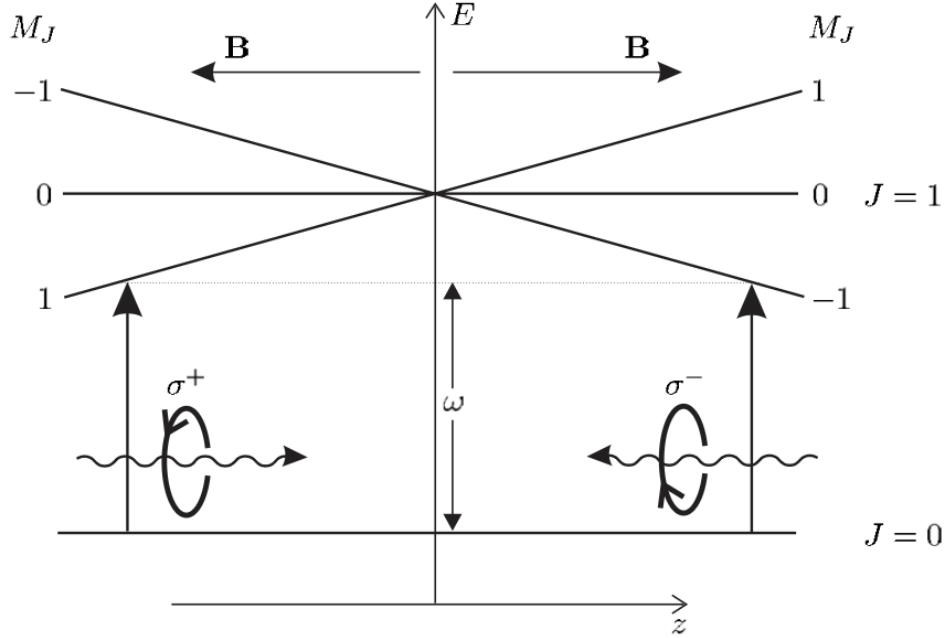


Figure 18: Magneto Optical Trap for a $J = 1$ system

results in the change in sign of m_j for the upper energy level. Light which excites the $|0,0\rangle \rightarrow |1,-1\rangle$ transition is denoted σ^+ and that which excites the $|0,0\rangle \rightarrow |1,1\rangle$ transition is denoted σ^- .

Consider an atom which moves from $z = 0$ to some $z > 0$. The Zeeman shift introduced by the magnetic field brings the laser light into resonance with the $|0,0\rangle \rightarrow |1,-1\rangle$ transition, increasing the radiation force to the left.

The scattering force acquires a position dependence:

$$F_{\pm} = \frac{\pm \hbar k \Gamma}{2} \frac{I}{2I + I_{sat} \left[1 + 4 \left(\frac{\Delta_{\mp} v_z k - b' |z|}{\Gamma} \right)^2 \right]} \quad (176)$$

Where we define $b' = m_j g_J \mu_B b / \hbar$, and b as the modulus of the magnetic field gradient.

For small velocities ($kv_z < \Gamma$) and displacements ($b' |z| < \Gamma$) the force simplifies:

$$F_{\pm} = -\alpha v_z - \beta z \quad (177)$$

$$\beta = -\frac{b' \alpha}{k} \quad (178)$$

Here, β acts like a spring constant and α a friction constant. The motion is of an overdamped oscillator.

A MOT can hold $\sim 10^{10}$ atoms in $\sim 1\text{mm}^3$ at around the Doppler temperature. The capture velocity is also $\sim 10\text{-}100$ times larger than that of optical molasses. The trap can therefore be loaded from room temperature.

11.2 Cycling Transitions

Consider the following problem: in Cs we drive the cooling transition $6^2\text{S}_{1/2} \rightarrow 6^2\text{P}_{3/2}$ from $F = 4$ to $F = 5$. The selection rules (that $\Delta F = 0, \pm 1$) imply that $F' = 5$ can only decay back to $F = 4$. However, since the cooling transition is slightly red de-tuned, the $F' = 4$ or even $F' = 3$ states could also be excited, which can decay back to $F = 4$ or $F = 3$. The decay of atoms to $F = 3$ implies we lose them from the cooling cycle. A re-pumping laser is used to return them to $F = 4$.

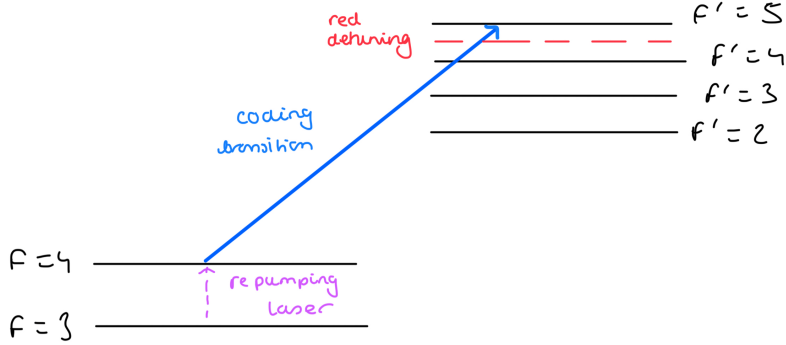


Figure 19: The requirement for re-pumping lasers

12 Lecture 12

12.1 Sub-Doppler Cooling/Sisyphus Cooling

It is actually possible to cool atoms to temperatures below the Doppler limit. The derivation of T_D assumes that alkali atoms behave as ideal two-level systems without accounting for Zeeman substructure. A more detailed analysis reveals an additional mechanism that allow atoms to dissipate more energy and reach lower temperatures.

Study Figure (20). Part (a) shows the upper level as the excited state ($J = 3/2$) of the cooling transition, and the lower level as the ground state ($J = 1/2$). The numbers on the arrows indicate relative transition probabilities (their derivation is not required).

The upper panel of (b) shows the interference of 2 counter propagating laser beams with orthogonal linear polarization. This creates a polarization gradient. The gradient causes the m_J states to separate in energy. This is called the AC stark effect. The energy separation is show in panel (d).

Now study panels (c) and (d). At the σ^+ position (indicated by the double arrow) the $m_J = -1/2$ state atoms "climb the hill" and lose kinetic energy. The atoms in this state then absorb the σ^+ radiation and are excited to $m_{J'} = +1/2$. The atoms then spontaneously decay to $m_J = +1/2$, which is in a "valley" of the ground state. Kinetic energy of the system has been removed by the emitted photon. Figure (21) shows the cycle of absorption and spontaneous emission in more detail.

This process only works for already cold atoms, as they must move slowly enough to respond to the optical potential. The capture velocity is lower than for Doppler cooling. Cooling stops when atoms no longer have enough kinetic energy to climb the potential hills. The final temperature can be estimated from the energy difference between the hills and valleys (derivation not required).

$$k_B T_{sis} = \frac{\hbar \Omega^2}{4\Delta} \propto \frac{I}{|\Delta|} \quad (179)$$

There is a fundamental limit to this cooling, reached when the energy lost moving from hill to valley equals the energy gained from the recoil of a spontaneously emitted photon. This is the **recoil limit**.

$$k_B T_r = \frac{\hbar^2 k^2}{M} \quad (180)$$

Where each degree of freedom has energy $E_r = \frac{1}{2} k_B T_r$

12.2 The Atomic Fountain Clock

See Figure (22). The clock works by the following mechanism:

- The atoms are launched into a moving frame by bringing the upward optical molasses beam closer into resonance with the atoms and tuning the downward beam further from resonance.

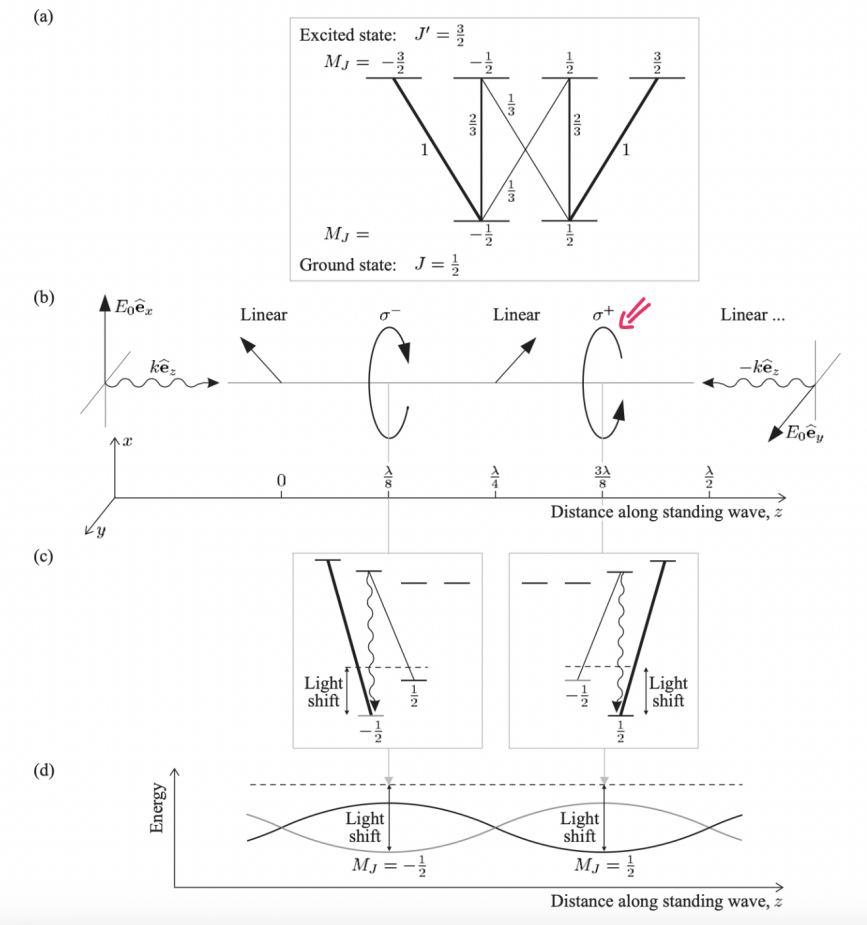


Figure 20: The Sisyphus Cooling mechanism

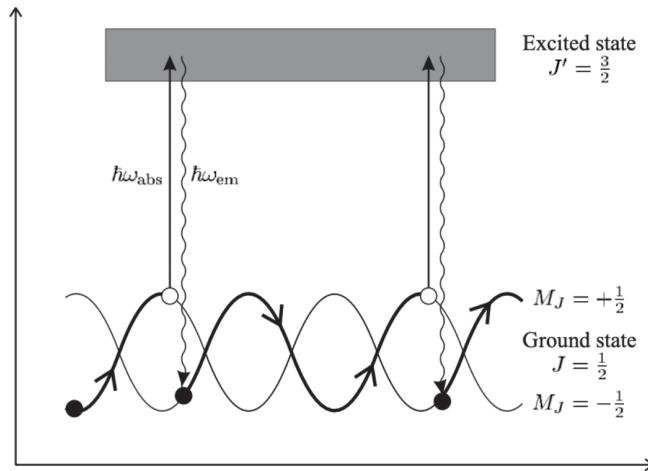


Figure 21: The cycle of absorption and spontaneous emission

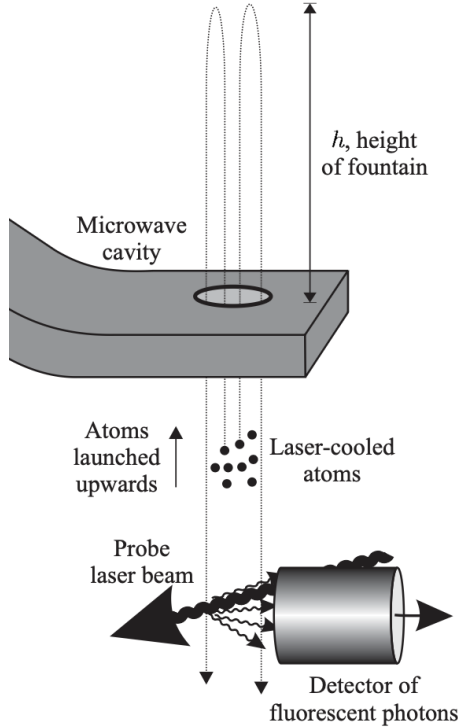


Figure 22: An atomic fountain clock

- The beam passes the microwave cavity, where it receives the first Ramsey $\pi/2$ pulse.
- The beam falls under gravity.
- The beam passes the microwave cavity for a second time and receives the second Ramsey $\pi/2$ pulse.
- The number of atoms in the excited state of the clock transition is then measured.

Note that it is required to cool the atoms before they enter the clock, otherwise they wouldn't make it 'back down'.

The Cs-133 clock transition from $|F = 3, m_F = 0\rangle \rightarrow |F = 4, m_F = 0\rangle$ is used as the **primary frequency standard**. It is a low frequency, Zeeman insensitive transition with a weak dipole moment (and therefore small natural broadening).

12.3 The Moving Molasses

To launch the atoms into a moving frame, the frequency shifts demonstrated in Figure (23) are made.

Once the atom begins to move upward, we would like them to return to the typical optical molasses set up, with each frequency red de-tuned to the dashed line. This is done naturally via the Doppler shift. For example, the upward pointing beam which is **deliberately blue de-tuned** is then **red de-tuned** by the upward motion of the atom.

Recalling the red de-tuned Doppler shift:

$$\omega_a = \omega_l \left(1 - \frac{v_z}{c} \right) \quad (181)$$

For the overall frequency to lie on the dashed line, we require:

$$\frac{\Delta_{mm}}{2} - \frac{v_z \omega_l}{c} = 0 \quad (182)$$

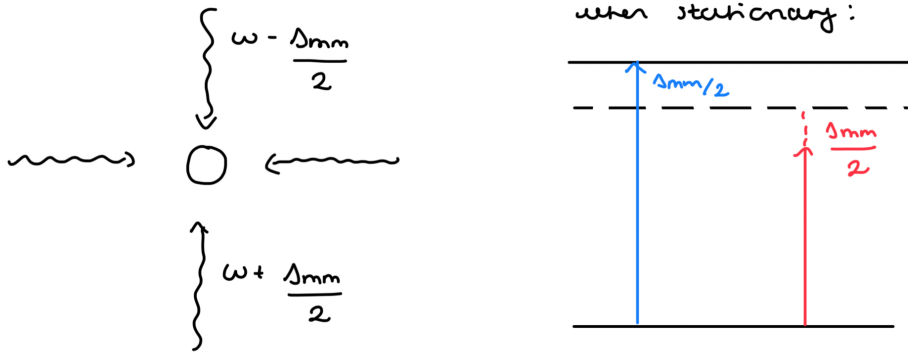


Figure 23: Kick starting the moving molasses

12.4 Clock Dimensions and Precision

If we set for example $\Delta_{mm}/2 = 5.0$ MHz, we obtain an upward launch of $v_0 = 4.3$ ms⁻¹. From this and a suvat equation we can obtain the height of the clock:

$$v^2 = v_0^2 - 2gh \implies h = \frac{v_0^2}{2g} = 94.2 \text{ cm} \quad (183)$$

The interaction time can then also be determined:

$$v = v_0 - gt \implies v_0 = gt = \sqrt{2gh} \implies t = \sqrt{\frac{2h}{g}} \implies \tau = 2\sqrt{\frac{2h}{g}} \quad (184)$$

Atomic fountain clocks can obtain a fractional uncertainty of $\sigma = 10^{-16}$. This is better than the atomic beam clock due to the longer interaction time. At this level of precision, all sources of systematic error are accounted for in an **uncertainty budget**.

13 Lecture 13

13.1 Precision

Recall the fractional uncertainty in an atomic clock is given by:

$$\sigma = \frac{\Delta\omega}{\omega} \sqrt{\frac{\tau_c}{N\tau}} \quad (185)$$

Therefore, increasing either the number of atoms or the integration time improves the precision. These approaches are employed in the **optical lattice clock** and the **trapped ion clock**, respectively.

The formula also shows that higher-frequency transitions improve precision. These are typically optical transitions. While we previously ruled them out due to their usually large radiative broadening, certain special optical transitions—known as **forbidden** transitions—have exceptionally long lifetimes and are therefore suitable for high-precision clocks.

13.2 The Optical Frequency Comb

We use lasers to drive the optical transitions in atomic clocks. We therefore need to be able to measure the exact frequency the laser excites. To do this we use frequency combs.

Frequency combs are the Fourier transform of the femto-second pulses produced by lasers, see Figure (24).

When analyzing the frequency comb, we can measure relative frequencies, but not absolute since we don't know the frequency of the first node. This is the carrier envelope offset, demonstrated in Figure (25).

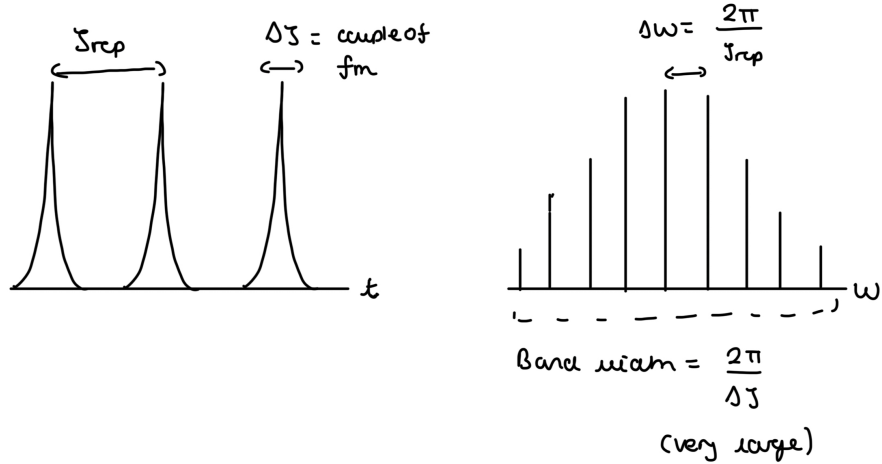


Figure 24: Femto-second pulses (RHS) and the Fourier Transform in frequency space (LHS)

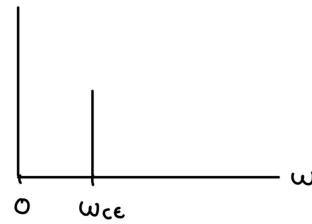


Figure 25: The carrier envelope offset

The frequency of the n^{th} comb tooth is:

$$\omega_n = \omega_{CE} + n\Delta\omega \quad (186)$$

ω_{CE} can be found through the "octave spanning" comb. Figure (26).

The frequency of the beat measured at the photo-diode interface is given by:

$$\omega_{\text{beat}} = 2\omega_n - \omega_{n'} = \omega_{CE} \quad (187)$$

Now we can accurately compute the frequency of every node and we have a 'frequency ruler'.

13.3 The Excitation Laser

The frequency uncertainty of the excitation laser must be smaller than the width of the Ramsey fringe. Therefore, it must be in the mHz range. Such ultra-stable lasers are achieved using techniques like mode-locking.

Figure (27) shows a simplistic ultra stable laser. The cavity only supports frequencies corresponding to $n\lambda/2$. The relationship

$$\frac{\Delta f}{f} = \frac{\Delta L}{L} \quad (188)$$

defines the relationship between the laser frequency, cavity length and their uncertainties.

For example, if we needed $\Delta f = 0.1$ Hz for a laser of frequency $f = 6 \times 10^{14}$ Hz supported by a cavity length of $L = 0.1$ m we obtain $\Delta L = 1.6 \times 10^{-17}$ m which is tiny! Cavities are therefore highly engineered. They are made from ultra-low thermal expansion materials and housed in a vacuum to minimize vibrations.

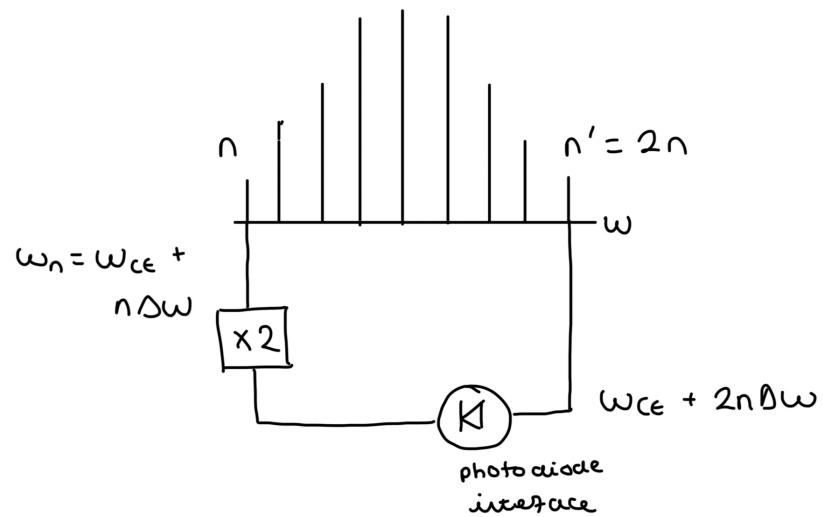


Figure 26: The Octave spanning comb

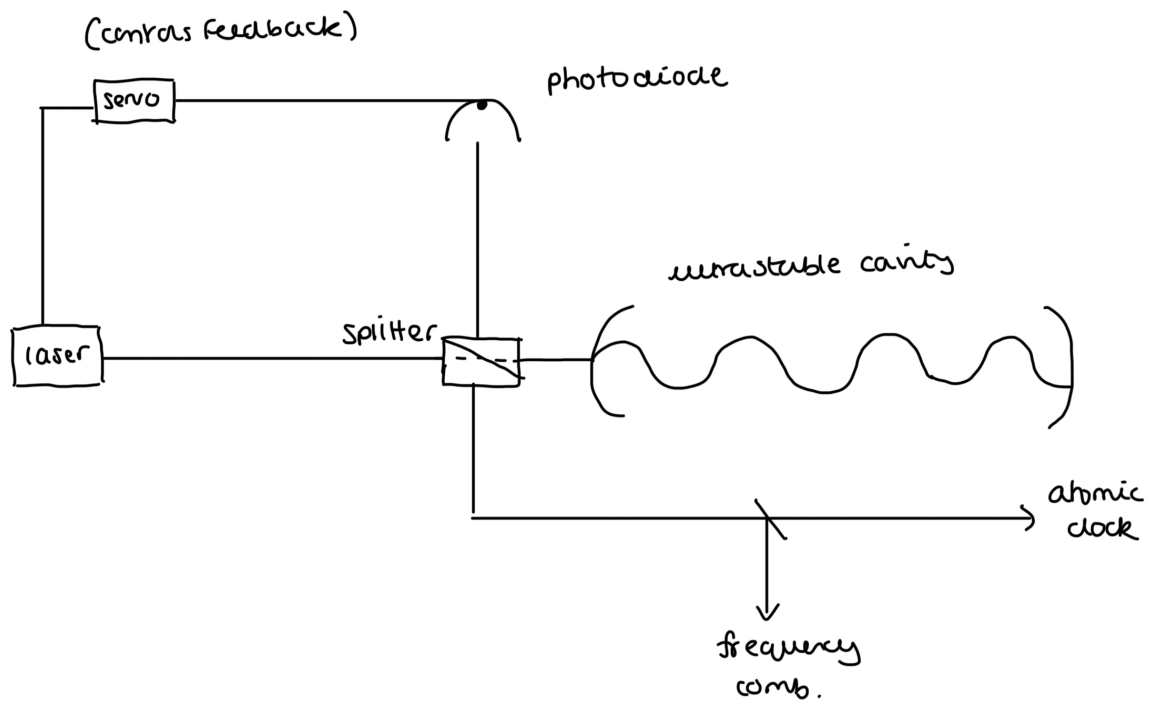


Figure 27: A simplistic ultra-stable laser used in atomic clocks

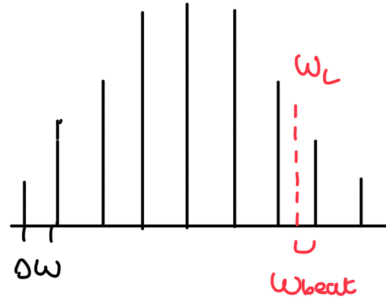


Figure 28: Measuring the laser frequency ω_l

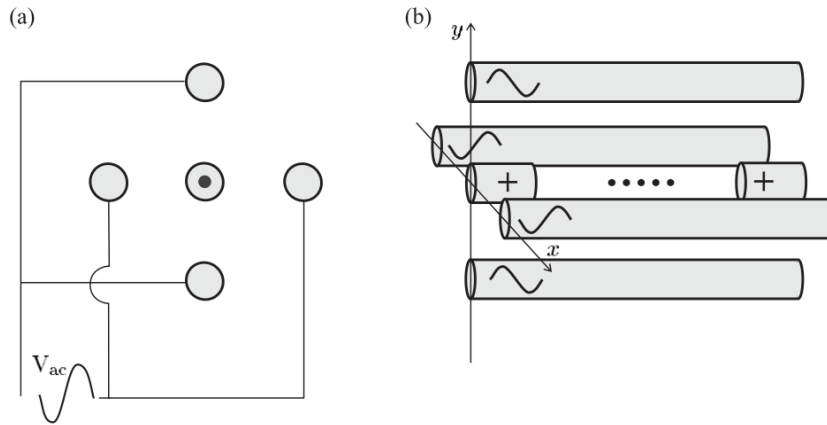


Figure 29: A Paul Trap

To measure the clock laser frequency, we interfere the clock laser with the closest comb mode and measure the beat frequency. See Figure (28). The laser frequency is given by:

$$\omega_l = \omega_{CE} + n\Delta\omega \pm \omega_{beat} \quad (189)$$

Note that we must know the laser frequency to within $\Delta\omega/2$ such that we can accurately identify the value of n .

14 Lecture 14

In this lecture we study ion traps, which are used to achieve clocks with a long integration time.

Ion traps can be loaded from room temperature since the Coulomb force is very strong. The kinetic energy an ion would need to escape a modest electric field of $\sim 10^5 \text{V/m}$ is equivalent to a thermal temperature of $6 \times 10^6 \text{K}$.

14.1 Earnshaw's Theorem and the Linear Paul Trap

Trapping with electrostatic potentials involves a subtle complication. According to Earnshaw's Theorem, static electric fields cannot produce a stable equilibrium point in three dimensions; that is, no local maxima or minima can exist—only saddle points. To achieve stable trapping, we use time-varying electric fields which result in a rotating saddle point.

The most common ion trap is the Paul trap, see Figure (29). The rod along z is a DC field and those along each x and y oscillate 180° out of phase, creating quadrupole and trapping in the xy plane. The ions are ultimately confined along the z axis. The underlying electrodynamics is not on the syllabus.

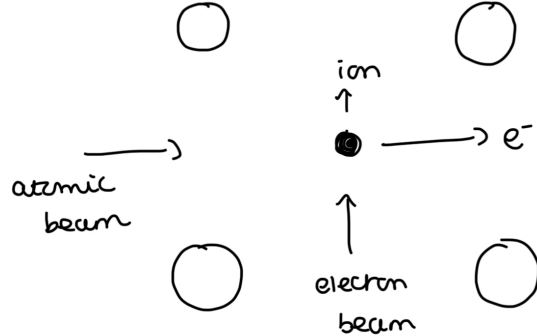


Figure 30: The loading of the ion-trap

The motion of an ion in a linear Paul trap along the i axis (in Figure (29) this is the z axis) is described by the Mathieu Equation:

$$\frac{d^2i}{dt^2} + (a_i + 2q_i \cos(\Omega_{RF}t)) = 0 \quad (190)$$

$$a_i = -\frac{8V_{DC}}{\Omega_{RF}^2 d_i^2} \left(\frac{q}{m} \right) \quad (191)$$

$$q_i = \frac{4V_{AC}}{\Omega_{RF}^2 d_i^2} \left(\frac{q}{m} \right) \quad (192)$$

Here, Ω_{RF} is the angular frequency of the applied AC voltage. V_{DC} is the static voltage applied to the end-cap electrodes, and V_{AC} is the amplitude of the oscillating (AC) voltage. The quantity d_i denotes the characteristic trap dimension along the i -th direction and q/m is the charge to mass ratio of the ion. Note that only a certain range of parameters will give trapping for a given q/m .

The trapped ions' motion is of a harmonic oscillator with angular frequency:

$$\omega_{trap} = \sqrt{\frac{q_i^2}{2} \Omega_{RF}^2 - a_i} \quad (193)$$

This is normally a few MHz.

In experiment, the trap is loaded through ionizing atoms from a weak beam, see Figure (30). The fast electrons leave the trap, while the ion is in a stable trajectory.

14.2 Doppler Cooling in Ion Traps

To do precision measurements, we require an ion to be cold. We use Doppler Cooling, but only with one laser beam because the ion oscillates back and fourth in the trap. As the ion moves toward the laser it is Doppler shifted into resonance and scatters more photons, decelerating it. See Figure (31).

14.3 Resolved Sideband Cooling

Once ions have been cooled by to the Doppler temperature, they are quantum harmonic oscillators. Each atomic level has its own vibrational states. The vibrational levels are the same for both the ground and excited states as they only depend on q/m .

The system can be cooled further if the vibrational levels are resolved: $\omega_{trap} > \Gamma$. This is called **sideband cooling**. See Figure (32a). The energy of the system is reduced by firing laser light of a frequency $\omega_l = \omega_0 - \omega_v$ at the ion, where ω_v is the vibrational frequency. The ion transitions to the upper electronic state, with a vibrational quantum number $v' = v - 1$. This excited state decays back to the ground state. The possible changes in vibrational quantum numbers are $\Delta v = 0, \pm 1$ but

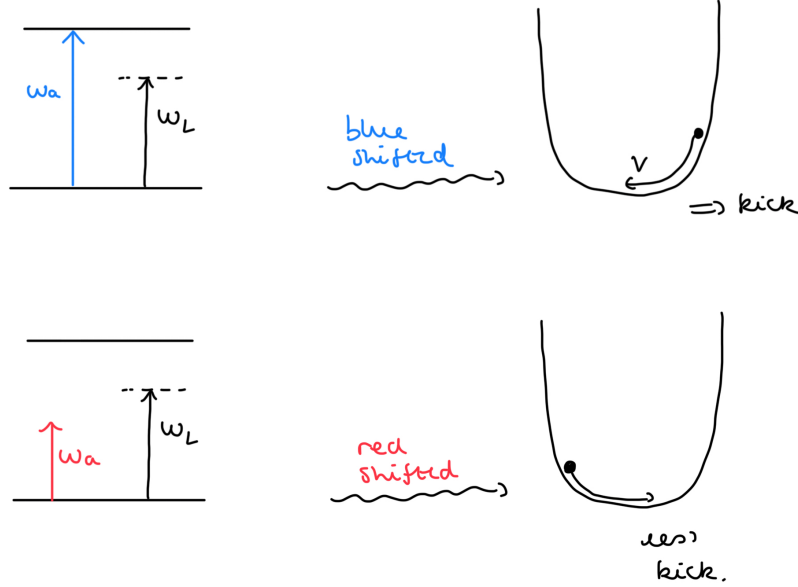


Figure 31: Doppler Cooling in an ion-trap

$\Delta v = 0$ is the most probable. Hence, on average the ion returns to the ground electronic state in a lower vibrational level than it started.

The cooling continues until the atoms have been driven to their lowest vibrational level. An ion in $v = 0$ no longer absorbs radiation of frequency $\omega_l = \omega_0 - \omega_v$. To experimentally verify a system of ions is in this lowest ground state, frequencies of $\omega_l = \omega_0 - \omega_v$ and $\omega_l = \omega_0 + \omega_v$ are applied to the system. As shown in Figure (32b), there is a much larger absorption signal at the upper-sideband than the lower-sideband, implying most ions are in the $v = 0$ state.

Technically, the transitions which change vibrational quantum number shouldn't be allowed if the electron is a point particle, since they are orthogonal states. However, if we remove the dipole approximation and allow the electron to have a spatial extent of

$$z_0 = \sqrt{\frac{\hbar}{2m\omega_{trap}}} \quad (194)$$

the transitions are allowed. The factor by which the probability of a $v = \pm 1$ transition is smaller than a $v = 0$ transition is given (without proof) by:

$$\eta^2 = (kz_0)^2 = \frac{\omega_{recoil}}{\omega_{trap}} \quad (195)$$

where ω_{recoil} is the angular frequency associated with the energy transfer from photon to ion.

14.4 The Lamb-Dicke Regime

η in the above equation is the Lamb-Dicke Parameter. In the Lamb-Dicke regime: $\eta \ll 1$, the scattered photons do not change the ions' vibrational state. If $v = 0$, the 1st order Doppler shift is removed as the particle (pretty much) isn't moving. An ion therefore approximates an **isolated unperturbed particle at rest**. We are therefore able to keep them trapped for days, allowing a very long integration time.

15 Lecture 15

15.1 Ion Trap Clocks

The requirements on atomic structure to build an accurate atomic clock are shown in Figure (33).

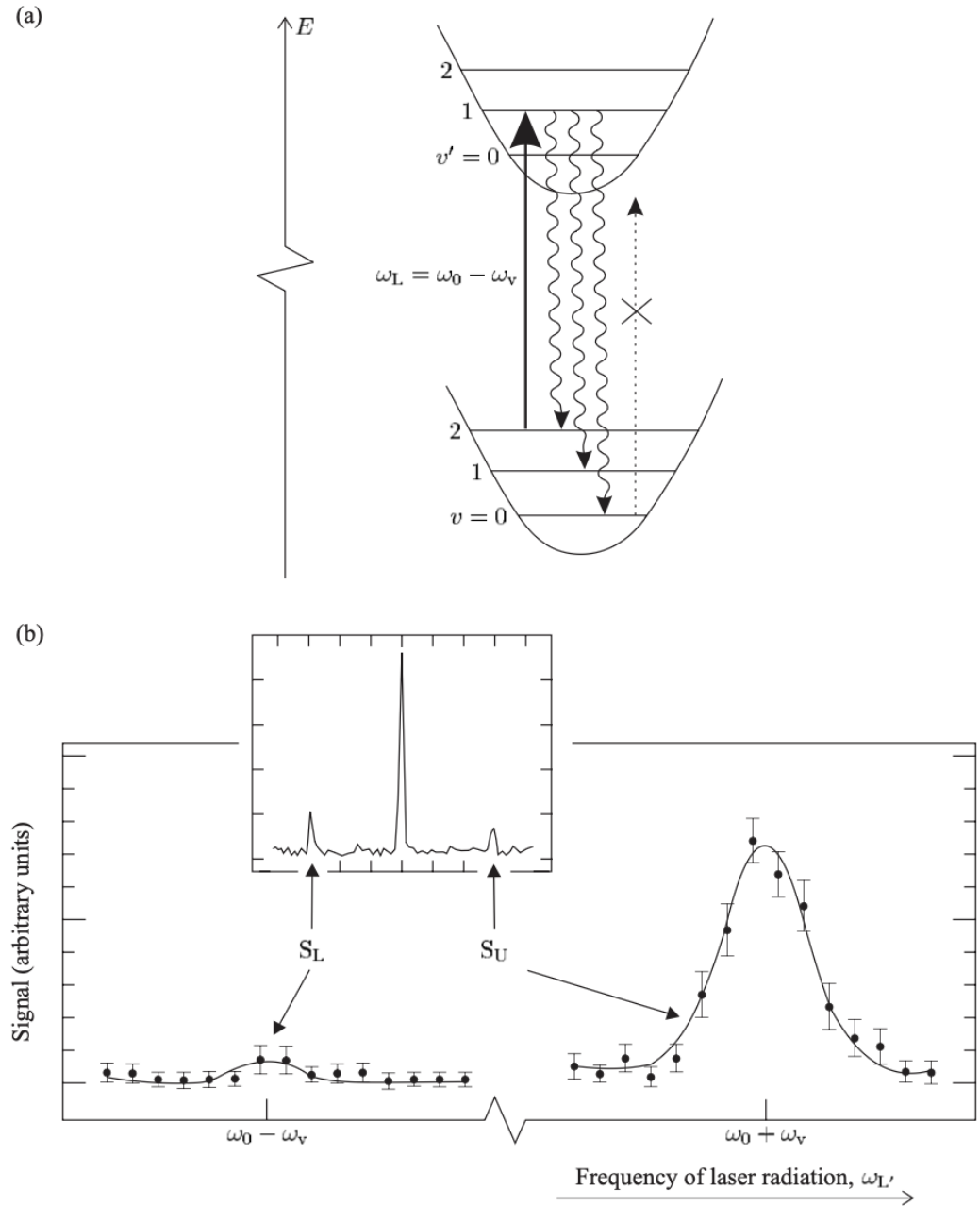


Figure 32: Side-band cooling to obtain a motional ground state

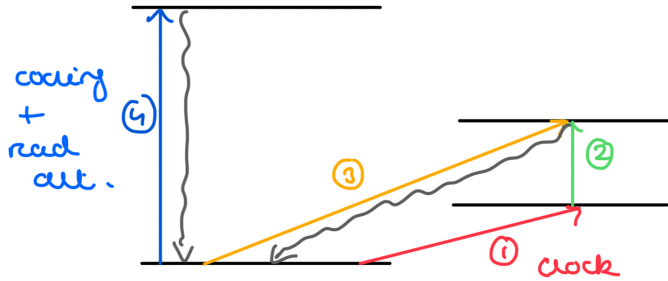


Figure 33: Transitions in an atomic clock. The colored lines are the driven transitions and the gray are spontaneous decays.

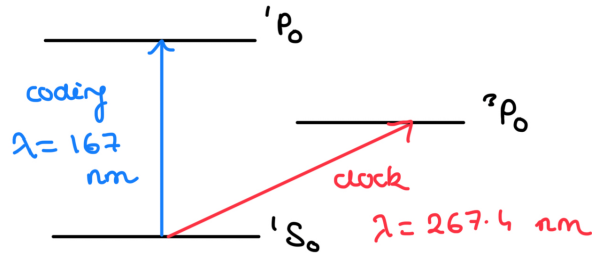


Figure 34: The clock and cooling transitions of an Al⁺ ion

1. Transition 1 is the clock transition. We would like $\Gamma \sim 2\pi$ Hz.
2. Transition 2 is a transition help return the ion to its ground state, after the required measurement time.
3. Transition 3 is a cooling transition, it would ideally have a smaller Γ than (4) such that it can cool to a lower $T_D = h\Gamma/2k_B$.
4. Transition 4 is the strong optical cooling and readout transition.

Each of these transitions must have wavelengths accessible through laser technology. There are actually only a few atomic candidates!

The processes of accessing the clock frequency is as follows:

- Drive a π pulse on the clock transition.
- Drive the **optical** cooling transition and record the **fluorescence**.
 - If the ion was excited into the clock state, it is in a **shelved** state and does not connect to the cooling transition. It therefore does not fluoresce.
 - If the ion remained in the ground state it scatters a photon on the cooling transition, we therefore see fluorescence.

15.2 The Aluminum Logic Clock

The Al-27+ ion has a very narrow clock transition between the 1S_0 and 3P_0 state, see Figure (34). This transition is **doubly forbidden** under selection rules since $\Delta S = 1$ (it should be 0) and $\Delta J = 0$. This makes the transition extremely narrow, with a line width:

$$\Gamma = 2\pi \cdot 8 \text{ mHz} \quad (196)$$

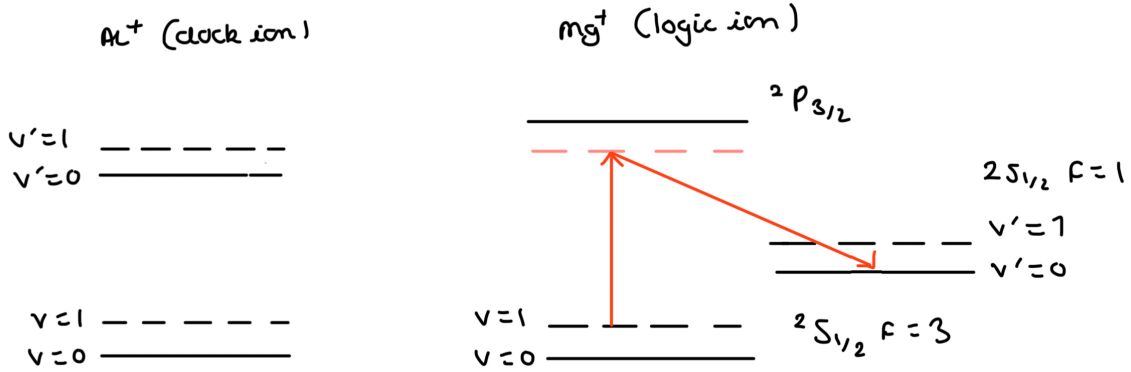


Figure 35: The atomic structure in the Al+ Mg+ logic ion clock

However, there is a problem: the available cooling transition is at 167 nm and cannot be driven by laser technology. We need a method to detect the Al⁺ transition indirectly. This uses a second ion, ²⁵Mg⁺, known as the logic ion.

The clock (Al⁺) and logic (Mg⁺) ions are trapped together and their motional states coupled such that they share a common ground state vibrational mode. This is done through sympathetic cooling, where the Mg⁺ ion is cooled with lasers and the Al⁺ ion is cooled through collisions with it.

The atomic structure of each Al⁺ and Mg⁺ is shown in Figure (35). It is necessary to drive a Raman transition (one which involves 2 photons and an unpopulated intermediate state) from $|^2S_{1/2}, F = 3, v = 1\rangle \rightarrow |^2S_{1/2}, F = 1, v = 0\rangle$ on the logic ion. This is because a direct transition would involve $\Delta F = 2$, which is forbidden. If Raman transitions couple to 2 long-lived states they have very narrow line-widths. The QM logic of the clock is demonstrated in Figure (36).

The logic is then:

- The system starts in the state:

$$|\downarrow\rangle_c |\downarrow\rangle_l |0\rangle_m \quad (197)$$

A $\pi/2$ pulse is then driven on the clock ion.

- The system is now in a superposition state

$$(\alpha |\downarrow\rangle_c + \beta |\uparrow\rangle_c) |\downarrow\rangle_l |0\rangle_m \quad (198)$$

If the superposition is perfect, $\alpha = \beta$. A π pulse is then driven on the clock ion with $\omega = \omega_{12} - \omega_{trap}$, forcing it into a superposition of motional states.

- Because the motional states are coupled, each ion experiences this superposition. The quantum states is:

$$|\downarrow\rangle_c |\downarrow\rangle_l (\alpha |0\rangle_m + \beta |1\rangle_m) \quad (199)$$

We then make a Raman π pulse on the logic ion.

- The π pulse forces the motional ground state. The system is now in the state:

$$|\downarrow\rangle_c (\alpha |\downarrow\rangle_l + \beta |\uparrow\rangle_l) |0\rangle_m \quad (200)$$

We then drive a logic transition between $^2S_{1/2}, F = 3$ and $^3P_{3/2}$. When the clock laser is on resonance, the averaged fluorescence over many experiments is reduced, since the logic ion has a probability to exist in $F = 1$.

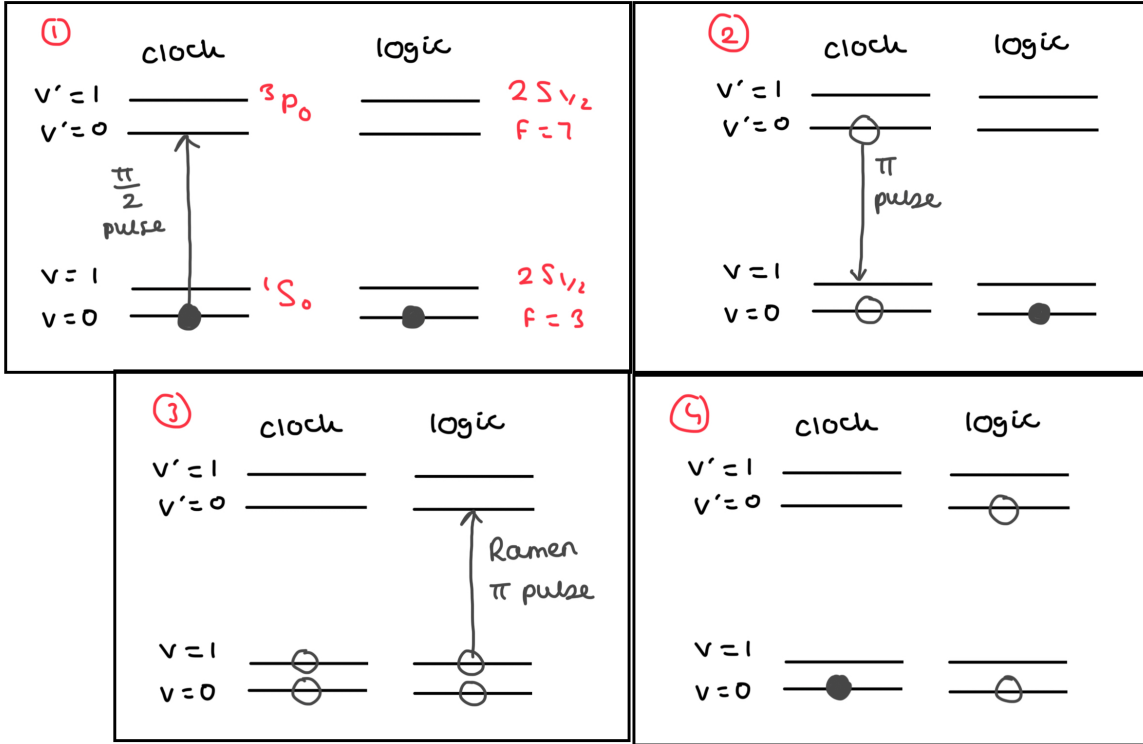


Figure 36: The Quantum Mechanics of the Aluminum logic ion clock

16 Lecture 16

16.1 Dipole Trapping

From electrostatics, we know that placing a charged rod near a small dust particle induces an electric dipole in the particle, which causes it to be attracted to the rod. A similar principle can be used to trap atoms. If an atomic dipole can be induced at the frequency of an external electromagnetic field, the atom can be held in place. To generate a strong, oscillating electric field, a laser can be focused through a lens and the atom positioned at the focal point.

This is known as an **optical dipole trap**. The trapping is much weaker than that in the ion trap, since the attractive force on the low-potential part of the dipole is only slightly larger than the repulsive force on the high potential part. We therefore require **laser cooled atoms**.

16.2 The Dipole Potential

Say we focus a time varying monochromatic laser, where the electric field takes the form:

$$\vec{E}(\vec{r}, t) = \hat{e} E_0(\vec{r}) \frac{[e^{-i\omega t} + e^{i\omega t}]}{2} = \hat{e} E_0(\vec{r}) \cos(\omega t) \quad (201)$$

We assume that the electric dipole take the form:

$$\vec{d}(\vec{r}, t) = \hat{e} d_0(\vec{r}) \frac{[e^{-i(\omega t+\phi)} + e^{i(\omega t+\phi)}]}{2} = \hat{e} d_0(\vec{r}) \cos(\omega t + \phi) \quad (202)$$

where the phase factor ϕ is added to show the response is not instantaneous. The Electric field and dipole are related through the polarizability $\alpha(\omega)$:

$$\vec{d} = \alpha(\omega) \vec{E} \quad (203)$$

The potential the dipole experiences is calculated through:

$$U_{dip} = - \int_0^E \vec{d}(\vec{E}') \cdot d\vec{E}' = - \int_0^E Re[\alpha(\omega)] \vec{E}' \cdot d\vec{E}' = -Re[\alpha(\omega)] \frac{E^2}{2} = -\frac{1}{2} \langle \vec{d} \cdot \vec{E} \rangle = -\frac{1}{2\epsilon_0 c} Re[\alpha(\omega)] I(\vec{r}) \quad (204)$$

This is known as the **light shift**. The force on the dipole is therefore:

$$\vec{F}_{dip} = -\nabla U_{dip}(\vec{r}) = \frac{1}{2\epsilon_0 c} Re[\alpha(\omega)] \nabla I(\vec{r}) \quad (205)$$

16.3 Balance in the Dipole trap

To construct an effective optical trap, it is essential that the trapping potential is sufficiently **deep** to confine the atoms, while the rate of **spontaneous emission** is kept as low as possible to avoid the heating caused by recoil. In the following, we examine how both the dipole trapping potential and the scattering rate depend on the laser de-tuning and intensity, and how to optimize these parameters to achieve strong confinement with minimal disturbance.

Without proof, the scattering rate as a function of polarizability is given by:

$$\Gamma_{sc}(\vec{r}) = \frac{1}{\hbar\epsilon_0 c} Im[\alpha(\omega)] I(\vec{r}) \quad (206)$$

The complex polarizability (derived from QM and not on the syllabus) can be substituted into each Γ_{sc} and U_{dip} to obtain the following expressions:

$$\Gamma_{sc}(\vec{r}) = \frac{3\pi c^2}{2\hbar\omega_{12}^2} \left(\frac{\omega}{\omega_{12}} \right)^3 \left(\frac{\Gamma}{\omega_{12} - \omega} + \frac{\Gamma}{\omega_{12} + \omega} \right)^2 I(\vec{r}) \quad (207)$$

$$U_{dip}(\vec{r}) = -\frac{3\pi c^2}{2\omega_{12}^3} \left(\frac{\Gamma}{\omega_{12} - \omega} + \frac{\Gamma}{\omega_{12} + \omega} \right) I(\vec{r}) \quad (208)$$

If in each of these equations, if we make the assumption that $\omega - \omega_{12} = \Delta \ll \omega_{12}$ then the terms simplify:

$$\Gamma_{sc}(\vec{r}) = \frac{3\pi c^2}{2\hbar\omega_{12}^2} \left(\frac{\omega}{\omega_{12}} \right)^3 \left(\frac{\Gamma}{\Delta} \right)^2 I(\vec{r}) \propto \frac{I}{\Delta^2} \quad (209)$$

$$U_{dip}(\vec{r}) = \frac{3\pi c^2}{2\omega_{12}^3} \frac{\Gamma}{\Delta} I(\vec{r}) \propto \frac{I}{\Delta} \quad (210)$$

Since Γ_{sc} must be minimized and U_{dip} must be maximized, the optimal configuration is to make both Δ and I large.

16.4 The Shape of the Potential

Often a laser beam takes on a Gaussian profile:

$$I(\vec{r}, t) = \frac{2P}{\pi W(z)^2} \exp\left(-\frac{2r^2}{W(z)^2}\right) \quad (211)$$

where P is the total power of the beam, $W(z)$ is the beam radius at a position z and r is the radial coordinate from the center of the beam. The beam waist evolution takes the form:

$$W(z) = W_0 \sqrt{1 + \left(\frac{z}{z_R}\right)^2} \quad (212)$$

Where W_0 is width of the beam at the focus and z_R is the Rayleigh length. When $r = W(z)$, the intensity of the beam is at e^{-2} of its maximal value. The Rayleigh Range is used to characterize the Gaussian beam. It is the distance along z from the focus at which the beam waist has increased by a factor of $\sqrt{2}$. It is equal to:

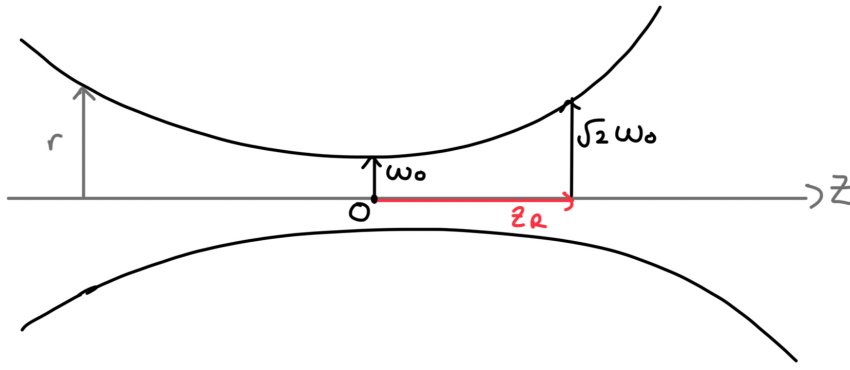


Figure 37: A Gaussian beam and its features

$$z_R = \frac{\pi W_0^2}{\lambda} \quad (213)$$

See Figure (37) to visualize the beam.

Assuming the trap laser is red-de-tuned ($\Delta < 0$), atoms are attracted to the intensity maxima of the beam, since the most negative potential is there, Equation (209). Around this focus, we make a Taylor expansion of the potential about $z = 0, r = 0$ after substituting the exponential form of $I(\vec{r}, t)$. See Workshop 8. We obtain:

$$U(r, z) = -U_{max} \left[1 - 2 \left(\frac{r}{W_0} \right)^2 - \left(\frac{z}{z_R} \right)^2 \right] \quad (214)$$

Hence, the potential has contributions from harmonic oscillators in the r and z directions. Comparing each component to the general harmonic oscillator potential $U = \frac{1}{2}m\omega^2x^2$ we obtain the radial and axial oscillation frequencies:

$$\omega_r = \sqrt{\frac{4U_{max}}{mW_0^2}} \quad (215)$$

$$\omega_z = \sqrt{\frac{2U_{max}}{mz_R^2}} \quad (216)$$

16.5 Optical Lattices

Optical traps have a much weaker confinement than ion traps, making it harder to reach the Lamb-Dicke Regime. In order to increase the confinement we use an **optical lattice**. This is formed by interfering counter propagating Gaussian laser beams. In 1D, this creates a periodic intensity pattern, and hence periodic potential.

From Optics (II) when two beams of wavelength λ interfere, the intensity varies as

$$I \propto 2 \cos^2(kz) = 2 \cos^2 \left(\frac{2\pi z}{\lambda} \right) \quad (217)$$

implying the lattice minima are spaced by $\lambda/2$. See Figure (38).

Accounting for this additional complexity, the potential becomes

$$U(r, z) = U_{max} \left(\frac{W_0}{W(z)} \right)^2 \exp \left(-\frac{2r^2}{W(z)^2} \right) \cos^2 \left(\frac{2\pi z}{\lambda} \right) \quad (218)$$

Here, the Gaussian envelope controls the radial confinement and the cosine squared term gives periodic wells in z .

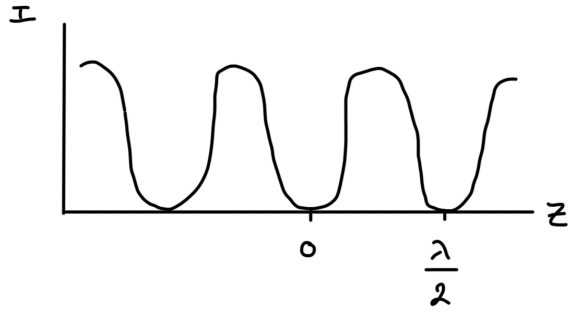


Figure 38: The intensity variation in an optical lattice

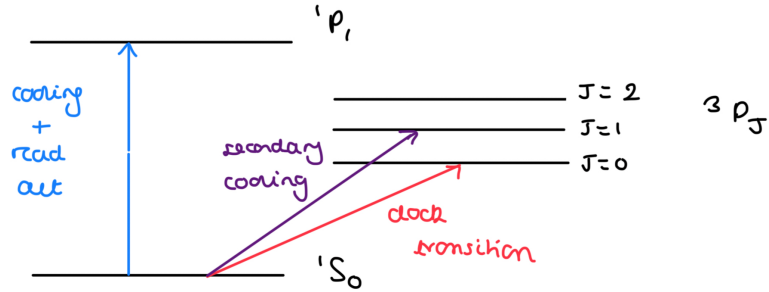


Figure 39: Strontium Clock Transitions

The optical lattice allows for tighter axial confinement and a deeper potential well. This is caused by the periodicity on the wavelength scale (due to the \cos^2 factor) and the fact that U_{max} is four times as large, since we now have 2 laser beams (we sum electric fields and square for intensity).

17 Lecture 17

Last Lecture! Here we study the Strontium Lattice Clock, the most precise atomic clock in existence.

17.1 The Atomic Structure of Strontium

Strontium is an Alkali Earth Metal with two valence electrons. Figure (39) shows the relevant clock states. There are 3 key transitions:

- The clock transition: From $5s^2 \ 1S_0 \rightarrow 5s^1 5p^1 \ ^3P_0$. This has a wavelength of $\lambda = 698$ nm and a linewidth of $\Gamma = 2\pi \cdot 26$ mHz. It is INCREDIBLY narrow.
- First stage cooling: From $5s^2 \ 1S_0 \rightarrow 5s^1 5p^1 \ ^1P_1$. This has a wavelength of $\lambda = 461$ nm and a linewidth of $\Gamma = 2\pi \cdot 32$ MHz. This is a strong, broad transition with a fast decay and subsequently high scattering rate.
- Second stage cooling: From $5s^2 \ 1S_0 \rightarrow 5s^1 5p^1 \ ^3P_1$. This has a wavelength of $\lambda = 689$ nm and a linewidth of $\Gamma = 2\pi \cdot 5$ kHz. This is a narrower transition which allows cooling to much lower temperatures (see the formula for T_D).

The clock transition is extremely narrow since it is **doubly forbidden**. $J = 0 \rightarrow J' = 0$ is forbidden and $\Delta S = 1$ (spin singlet to triplet) is also forbidden. It becomes allowed only via higher-order processes (e.g. magnetic dipole or electric quadrupole) making it extremely weak.

Strontium has many isotopes, but we use that of ^{87}Sr , which is fermionic. The Pauli Exclusion principle prevents them being at the same location. This reduces the frequency shifts caused by collisions.

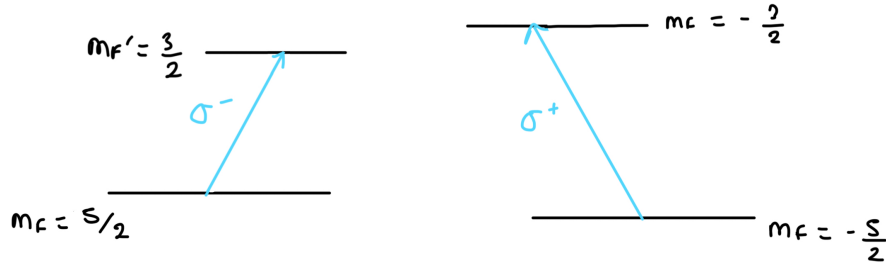


Figure 40: Averaging out the Zeeman shift effect.

17.2 The Experimental Sequence

The experimental sequence for an accurate reading is as follows:

- Step 1: Cool the atoms and load the MOT on the 461 nm transition. This achieves temperatures of $\sim 800 \mu\text{K}$.
- Step 2: Cool and load the MOT on the 689 nm transition. This transition has a narrower linewidth and therefore a lower Doppler Temperature: $T_D = \hbar\Gamma/2k_B \sim 1 \mu\text{K}$.
- Step 3: Load the Optical Lattice. Note that we don't keep atoms in the MOT since the scattering can cause a heating at very low temperature atoms and the EM fields can disturb the energy levels.
- Step 4: Sideband cooling and evaporation. Evaporation removes high energy atoms. The final temperature is $\sim 120 \text{nK}$. This is the Lamb-Dicke regime.

17.3 Accuracy and Precision

There are a couple more 'tricks' which allow such high accuracy and precision in clock readings.

Recall the AC Stark Shift, (or light shift) detailed in Equation (203). The optical lattice causes small energy level shifts, which depend on intensity and polarizability. The ground and excited states of atoms could experience different shifts, due to them having different polarizability, which would alter the clock transition. The solution is to use **magic wavelengths** such that the Stark Shift of the ground state is equal to that of the excited state. It then does not matter where in the trap the atom sits.

The clock states can experience weak Zeeman splitting in the presence of a magnetic field. To preserve the accuracy of the clock, we exploit the fact that the Zeeman shifts for symmetric stretched states (e.g., $m_F = \pm 1/2$) are equal in magnitude but opposite in sign. We drive transitions using σ^+ and σ^- circularly polarized light to access the corresponding excited states (e.g., $m_F = \pm 3/2$). By measuring the transition frequencies for both cases and taking their average, the first-order Zeeman shift is effectively canceled. This technique removes the dominant systematic magnetic field effect, improving the stability and precision of the clock. See Figure (40).

Strontium lattice clocks can hold up to 10^4 atoms per lattice site, and an average clock has ~ 100 lattice sites. This allows for the very small fractional uncertainty described in Lecture 13.

Overall the Strontium Lattice Clock is the most precise quantum technology in existence, with a fractional uncertainty of $\sigma = 10^{-16}$.